A REVIEW ON DEGRADATION MECHANISM AND LIFE ESTIMATION OF CIVIL STRUCTURES

A. Poonguzhali [*], H. Shaikh, R.K. Dayal and H.S. Khatak

Corrosion Science and Technology Division
Indira Gandhi Centre for Atomic Research
Kalpakkam – 603 102, India

ABSTRACT

Reinforced concrete (RC) is widely used in civil construction since it is the most versatile, economical and durable construction material of all times. Reinforcement corrosion has been widely reported to be one of the major durability problems, mainly when the rebar in the concrete is exposed to the chlorides, either contributed from the concrete ingredients or penetrated from the surrounding chloride-bearing environment. Carbonation of concrete or penetration of acidic gases into the concrete causes reinforcement corrosion. Besides these, factors related to the concrete quality, such as water/cement (w/c) ratio, cement content, impurities in the concrete ingredients, presence of surface cracks, etc. and those related to external environment, such as moisture, oxygen, humidity, temperature, bacterial attack, stray currents, etc., affect reinforcement corrosion. In this paper, a review is presented on the mechanisms of degradation of concrete, techniques used to monitor reinforcement corrosion, and empirical models and experimental methods to predict the remaining service life of structures.

Keywords: Reinforced Concrete (RC); Reinforcement corrosion; Mechanisms; Monitoring; Service life prediction

---

[*] Corresponding author:
Email: apoongs@igcar.gov.in;
Fax: +91 44 27480121

1.0 INTRODUCTION

Concrete is used as construction material. However, concrete is weak in tension in comparison to its compressive strength. Because of the low tensile strength of concrete, reinforcing steel bars are placed in regions of tension in a concrete member. This combination of concrete and steel provides a inexpensive and durable material that has been widely used in construction. As a construction material, concrete is used in a wide variety of applications. However, It is subjected to both physical and chemical deterioration. Abrasion and impact are examples of physical deterioration of reinforced concrete. Other physical deterioration processes, such as freezing of the solution within the pores in the concrete or crystallization of salts in the pores, may generate tensile forces within the concrete. In order to reliably fulfill its intended function, concrete must withstand attack by the environment to which it is exposed. Chemically induced deterioration of the concrete or corrosion of the reinforcing steel also occurs. Contamination of the concrete with sulphate ions can lead to various forms of sulphate attack of the cement paste in the concrete while the aggregate in the concrete may react with the highly alkaline cement to produce deleterious alkali-aggregate or alkali-silicate reaction. Chloride-induced steel corrosion is one of the major worldwide deterioration problems for steel reinforced concrete structures. The high alkaline environment of good quality concrete forms a passive film on the surface of the embedded steel, which normally prevents the steel from corrosion. However, under chloride attack, the passive film is disrupted or destroyed, and the steel spontaneously corrodes. The volume of the rust products is about four to six times larger than that of iron. This volume increase induces internal tensile stresses in the cover concrete and when these stresses exceed the tensile strength of the concrete, the cover concrete, a reinforced-concrete member may suffer structural damage due to loss of bond between steel and concrete and loss of rebar cross-sectional area. The rate of corrosion directly affects the extent of the remaining service life of a corroding reinforced concrete structure. The service life and utility of concrete depends on its transport properties of degrading ions. The ingress of potentially deleterious materials such as chlorides, sulphates, CO_2 and water by diffusion and capillary transport can lead to corrosion of steel reinforcement, resulting in reduced life of structure. Long life of these structures is essential for economic consideration. Predicting the service life of concrete is thus a subject of considerable interest. Empirical and physical models of degradation processes in concrete have been developed, but one complication in these approaches is that the material parameters on which these models are based continually change as the degradation occurs.

2.0 CONCRETE

Concrete is made from cement, aggregate, chemical admixtures, mineral admixtures and water. The active constituent of concrete is cement. The performance of concrete depends on the quality of the ingredients, their proportions, placement, and exposure conditions. The materials selected, such as cement type and admixture dosage, also play secondary roles by controlling other factors in early age drying and autogenous shrinkage **/1/.** Various admixtures are used in cement and construction industry to modify the properties of fresh and of hardened and hydrated cement pastes. Commonly admixtures in concrete can be classified with respect to their influence on the setting of cement. Admixtures which retard setting or hardening include sucrose, glycosides, phosphates, lignosulfonates and fruit acids. Admixtures which accelerate setting or hardening include amorphous aluminum hydroxides, soluble silicates, aluminates, aluminum sulfates, formiates, carbonates, soluble chlorides and organic components like triethanol amine **/2/.** Concrete plasticizers and super plasticizers include lignosulfonates, melamine sulfonates, naphthalene sulfonates, polycarboxylates (usually as sodium or alkali salts) and surfactants, which are added to concrete mixture in very small dosages. Their addition results in significant increase of the workability of the mixture, in reduction of water/ cement ratio or even of cement quantity **/3/.**

2.1 Constituents:

2.1.1 Cement

Portland cement is manufactured by crushing, milling and proportioning lime or calcium oxide, silica, alumina, iron and gypsum. The source of lime is provided by limestone, chalk, shells or calcareous rock and the sources of silica and alumina are argillaceous rock, clays and bauxite. The iron bearing materials are iron and pyrites. Ferric oxide not only serves as a flux, but also forms compounds with lime and alumina. The raw materials also contain small amounts of other compounds such as magnesia, alkalis, phosphates, fluorine compounds, zinc oxides and sulfides. The materials are proportioned to produce a mixture with the desired chemical composition and then ground and blended by dry and wet process. The materials are then fed through a kiln at 1426 °C to produce grayish-black pellets known as clinker. The clinker is cooled, pulverized and gypsum added to regulate setting time. It is then ground extremely fine to produce cement. Ground granulated blast-furnace slag is the granular material formed when molten iron blast furnace slag is rapidly chilled (quenched) by immersion in water. It is a granular product with very limited crystal formation, which is highly cementitious in nature and ground to cement fineness and hydrates like Portland cement. It can be substituted for cement on a 1:1 basis. The substitution of ground granulated blast furnace slag should be limited to 50 percent for areas not exposed to deicing salts and to 25 percent for concretes, which will be exposed to deicing salts. Addition of fly ash to concrete has become a common practice in recent years /**4**/. Fly ash is a finely divided residue resulting from powdered coal combustion and acts as a pozzolanic material. i.e. the particles react with water and lime to produce products that cause pore refinement which cause reduced permeability and reduction in calcium hydroxide content.

Properties of cement compounds:

a) *Tricalcium aluminate, C_3A:-* It liberates a lot of heat during the early stages of hydration, but has little strength contribution. Gypsum slows down the hydration rate of C_3A. Cement low in C_3A is sulphate resistant.
b) *Tricalcium silicate, C_3S:-* This compound hydrates and hardens rapidly. It is largely responsible for Portland cement's initial set and early strength gain.
c) *Dicalcium silicate, C_2S :-* C_2S hydrates and hardens slowly. It is largely responsible for strength gain after one week.
d) *Ferrite, C_4AF:-* This is a fluxing agent which reduces the melting temperature of the raw materials in the kiln. It hydrates rapidly, but does not contribute much to strength of the cement paste.

By mixing these compounds appropriately, manufacturers can produce different types of cement to suit several construction environments as given in Table 1 and Table 2.

The chemical composition and some physical and mechanical properties of cements are given in Table 3.

2.1.2 Water:

Water reacts chemically with cement to form the cement paste, which essentially acts as the "glue" (or binder) holding the aggregate together. The reaction is an exothermic hydration reaction. The water:cement ratio is an important variable that needs to be "optimized". High ratios produce relatively porous concrete of low strength, whereas too low a ratio will tend to make the mix unworkable. Fig.1 illustrates the relationship between W/C ratio and porosity.

Table 1

Compounds in Cement

Compound	Formula	% By Weight
Tricalcium aluminate	C_3A	10
Tetracalcium aluminoferrite	C_4AF	8
Dicalcium silicate	C_2S	20
Tricalcium silicate	C_3S	55
Sodium oxide	N	Up to 2 (N + K)
Potassium oxide	K	Up to 2 (N + K)
Gypsum	CSH_2	5

Table 2

ASTM Portland cement types

Type	Characteristics and Use
Type I, Ia, Standard	General purpose, Most residential purpose
Type II,IIa, Modified	Reduced heat of hydration, increased sulphate resistance
Type III, IIIa, High Early Strength	Gain strength in one to three days.
Type IV, Low Heat	Heat during hydration kept to a minimum; intended for large masses
Type V, Sulphate Resistant	Especially good for marine structures and soils with high alkali

Table 3

Physical, Chemical and Mechanical properties of cements **/7/.**

Chemical Composition	**Portland Cement**	**Slag Cement**
Sio_2	19.3	28.9
Al_2o_3	5.6	9.2
Fe_2o_3	3.5	2.2
Cao	63.6	47.4
Mgo	0.9	5.1
Na_2o	0.1	
K_2o	0.8	
So_3	2.9	1.7
Cl-	0.013	0.012
Loss on Ignition	2.8	0.4
Insoluble Residue	0.4	
Free CaO (%)	1.2	
Physical Properties		
Specific Gravity	3.15	2.96
Initial Setting Time (Min)	119	170
Final Setting Time (Min)	210	230
Volume Expansion (Mm)	1.00	
Specific Surface (M^2/Kg)	352	496
Compressive Strength (MPa)		
2 Days	27.2	18.0
7 Days	42.4	27.0
28 Days	52.7	48.0

2.1.3 Aggregates:

Aggregates are usually described as inert “filler” material of either the fine (sand) or coarse (stone) variety. The shape, size, density and strength of aggregate particles can vary significantly and can therefore influence the properties of the concrete. Aggregate represents a relatively high volume percentage of concrete, to minimize its cost.

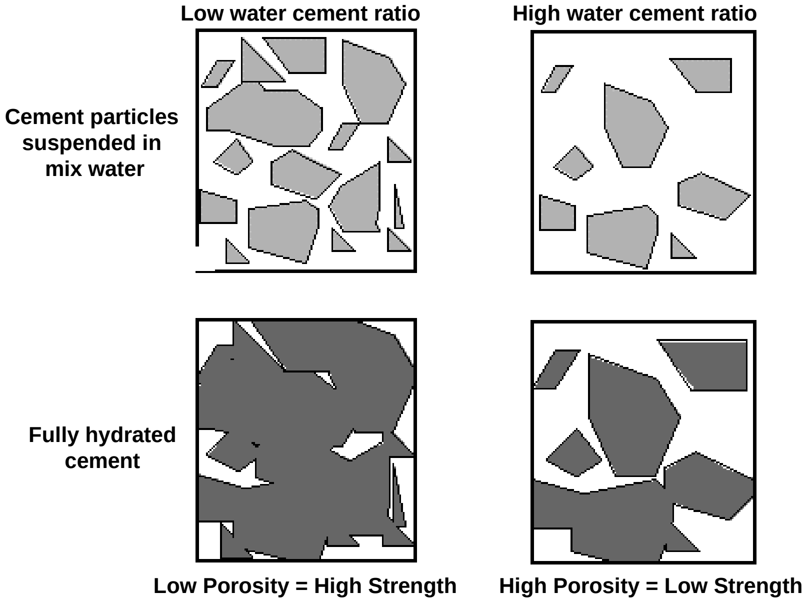

Fig. 1: Schematic drawings to demonstrate the relationship between the water/cement ratio and porosity**.**

2.1.4 Admixtures:

Admixtures are materials other than cement, aggregate, or water that are added to the batch of concrete immediately before or during mixing to impart desirable properties to it. Water-reducing admixtures permit the use of less water to give a concrete mix equal consistency that may result in a final product of greater strength, watertightness and durability. Air-entraining admixtures are used to increase the resistance of hardened concrete to cycles of alternate freezing and thawing and to improve the workability of the concrete mix. Accelerator admixtures are used to increase the early strength of concrete. Some accelerator admixtures contain chloride and should only be used for temporary construction. All admixtures should only be used when necessary.

2.2Fabrication:

2.2.1 Water to cement ratio:

It is well known that the reinforcing steel bar in concrete corrodes mainly due to chloride and sulfate attacks in marine environment. Traditionally, the performance of concrete used in marine environment depends on the concrete with a higher compressive strength and a lower permeability and it can be achieved by using low W/C ratio and an appropriate cementitious material. Decrease in W/C ratio results in reducing the cover thickness required for initial corrosion /**5**/. W/C ratio of higher than 0.42 is chosen to minimize the early stages of drying, hydration and effect of endogeneous shrinkage on strength and elastic property measurements as compared to W/C ratio of 0.8 which causes more rapid drying due to increase of the continuous capillary porosity /**6**/. There is an increase in uniaxial strength of concrete by 21% for W/C ratio of 0.45 and by 32% for W/C ratio of 0.8 but the strength decreases at the end of drying. Compressive and tensile strength of Portland cement mixtures decreases after wetting and drying cycles in sea water, while strength of slag cement mixtures increased slightly at W/C of 0.43 and 0.53 due to the effect of Na^+ and K^+ ions in sea water on pozzolanic reaction of slag /**7**/. Slag cement mixtures are considerably more resistant to chloride ingress than Portland cement mixtures at constant cement dosage and W/C ratio. Felekoglu *et al.* tested compressive strength of hardened self-compacting concrete (SCC) made of "Polycarboxylic-acid" superplasticizer /**8**/. Modulus of elasticity and splitting tensile strengths of specimens were determined at 28 days. Fig. 2 shows that a rapid strength development can be obtained by reducing the free water content and thereby W/C ratio.

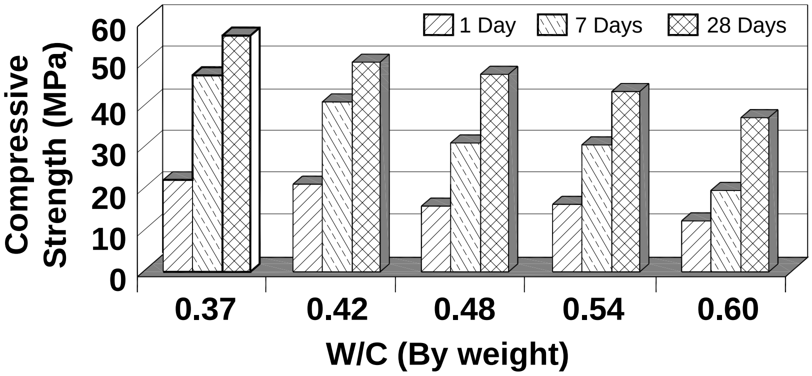

Fig. 2: Compressive strength development of concrete mixtures /**8**/.

2.2.2 Temperature of mixing:

The micro-structural modifications of cement based materials, namely physico–chemical transformations and thermal strains, which occur with temperature increase due to loss of water **/9/**. Aggregates expand continuously upon heating, whereas cement paste expands until 150 °C then shrinks above this temperature. This shrinkage is attributed to the loss of bounded water and, as a consequence, micro-cracks occur with a possible effect on porosity and permeability. The combination of strain incompatibilities and physico–chemical phenomena leads to a deep modification of the porous network which results in an increase in total porosity and a smoother distribution of pore sizes. Upon heating, the cement paste undergoes a continuous sequence of more or less irreversible decomposition reactions. The thermal decomposition of the cement paste can be understood by thermogravimetric analysis (TGA) and the deriveative thermogravimetric analysis (DTG) curves. This technique can be used to determine fire conditions and the consequent deterioration expected in the cement paste **/10/**.

- 30–105 °C: the evaporable water and a part of the bound water escapes. It is generally considered that the evaporable water is completely eliminated at 120 °C.
- 110–170 °C: the decomposition of gypsum (with a double endothermal reaction), the decomposition of ettringite and the loss of water from part of the carboaluminate hydrates take place
- 180–300 °C: the loss of bound water from the decomposition of the C-S-H and carboaluminate hydrates
- 450–550 °C: dehydroxylation of the portlandite (calcium hydroxyde)
- 700–900 °C: decarbonation of calcium carbonate

2.3 Properties of Concrete:

Workability: The concrete composition should be such that it is easily mixed, handled, transported and placed with vibrators without loss of homogeneity.

Strength: The strength of concrete is related to the amount of mixing water used (W/C ratio). Thus, the common field practice of adding more water to improve workability at a sacrifice in strength should be avoided. As shown in Fig. 3, the W/C ratio affects compressive strength much more than tensile and flexural strengths. Compressive strength increases with the age of the concrete. The hardening process begins at final set and continues indefinitely with favorable curing temperatures.

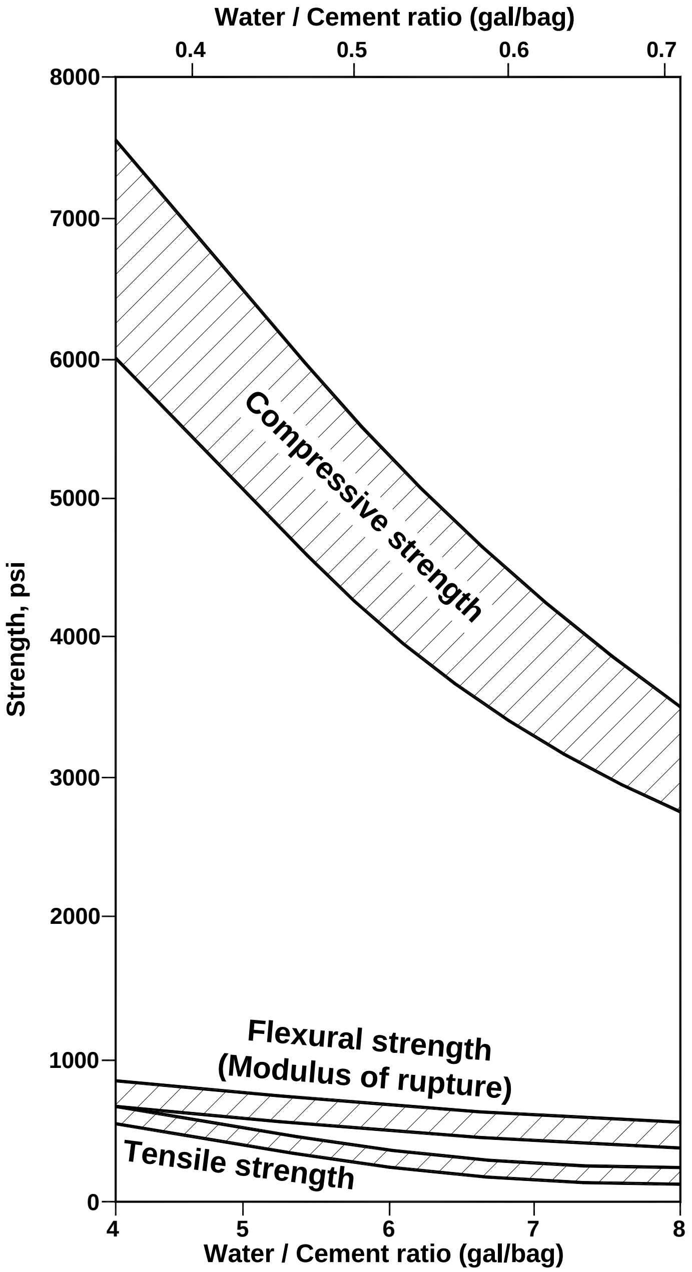

Fig. 3: Effect of water/cement ratio on 28 day compressive, flexural and tensile strengths.

Durability: A durable concrete will exhibit resistance to weathering, chemical deterioration and erosion. Concrete composition is the most important factor related to durability. The durability of concrete exposed to freezing and thawing conditions is enhanced by use of air-entraining admixtures.

Watertightness: Excess water in the concrete mix creates voids or cavities which increase permeability. Thus a proper W/C ratio is very important.

2.4 Rebars:

Reinforced concrete is a common building material for the construction of facilities and structures. While concrete has a high compressive strength, it has a very limited tensile strength. To overcome the limitations of tensile strength, reinforcing bars are used in the tension side of concrete structures. Steel rebars are effective and cost-efficient concrete reinforcement, but are susceptible to oxidation when exposed to aggressive agents like chlorides. Examples of such exposure include marine areas, regions where road salts are used for deicing and locations where salt contaminated aggregates are used in the concrete mixture. When properly protected from chloride ion attack, steel reinforcement can last for decades without exhibiting any visible signs of deterioration. However, it is not always possible to provide this kind of corrosion protection. Insufficient concrete cover, poor design or workmanship, poor concrete mix and presence of large amounts of aggressive agents can lead to corrosion of the steel rebar and cracking of the concrete.

Conventional ASTM B grade steel is the most widely used rebar material. However, a special grade of corrosion resistant thermomechanically treated steels (TMT Fe415) with the addition of alloying elements like Cr, Cu etc for improved strength and corrosion resistance is beneficial. Rebars made of stainless steels and nitrogen-containing steels, are proposed as they possess equal strength and toughness but better corrosion reistance with respect to chloride and CO_2 penetration through concrete structures.

2.4.1 Type of Rebar Specification :

IS:432 (Part I) – 1966 – Specification for mild steel and medium tensile steel bars and hard-drawn steel wire for concrete reinforcement.

IS:1786 – 1985 – Specification for high strength deformed steel bars for concrete reinforcement.

IS:226 – 1975 – Specification for structural steel (Standard quality)

IS:2062 – 1980 – Specification for structural steel (Fusion welding quality)

IS:13620:1993 – Fusion bonded epoxy coated reinforcing bars – specification.

British Standard BS 6744:2001 “Stainless steel bars for the reinforcement and use in concrete - Requirements and test methods”

ASTM A955/A995M: 2004 “Deformed and Plain Stainless Steel Bars for Concrete Reinforcement”

ASTM A1022 – 01 “Standard specification for deformed and plain stainless steel wire and welded wire for concrete reinforcement”

1) Stainless steel reinforcing bars:

Stainless steels exhibit higher corrosion resistance than ordinary black, galvanised or epoxy-coated rebars. Although the material costs are higher they may be used as an appropriate additional measure for the protection of concrete components with a high risk of corrosion. The suitability in a particular case may be judged on the basis of the life cycle costs. The avoidance of extensive repair work saves, in a sustainable way, not only financial, but also material resources. Additionally, the risks of repairs in respect to their effectiveness and durability can also be avoided by the use of stainless steel rebars. Stainless steels are used because of their good corrosion resistance and especially for concrete components that are exposed to chloride containing water. The resistance of stainless steels against pitting or crevice corrosion is improved by the elements like chromium, molybdenum and nitrogen. For stainless steel reinforcing bar applications, austenitic and duplex alloys have generally received the most attention. Cold rolled 304LN bars are prone to pitting while cold rolled 316LN bars, in contrast, maintain excellent corrosion behaviour along with very good mechanical properties. **/11/**.

The stainless steel rebar has the following potential advantages:

- inherently good corrosion resistance.
- reduced life cycle cost for concrete structures.
- good strength and ductility at all temperatures.
- good weldability.
- no coating requirement.
- no coating damage to repair.

- no “exposed” cut ends to coat or cover.
- capable of withstanding shipping, handling, bending.
- magnetic or non-magnetic, depending on the alloy specified.

2) Fiber reinforced polymer (FRP):

FRP composite rebar have the potential to address corrosion deficiency of steel rebars. FRP rebar can be used as non-prestressed reinforcement in concrete for members subjected to flexure, shear, and compression loadings. FRP composite rebars are totally resistant to chloride ion attack, offer a tensile strength of 1½ - 2 times that of steel, weigh only 25% of the weight of equivalent size steel rebar and are highly effective electromagnetic and thermal insulators. The thermal behaviour of concrete beams reinforced with Carbon Fibre Reinforced Polymer (Leadline) rebars is better than that of beams reinforced with steel. The Leadline reinforced beams show higher stiffness than the steel reinforced beams **/12/**. But the glass fibre strength and modulus is reduced by exposure to alkali and by testing at elevated temperatures within the range 20– 120 °C. The nature of the resin matrix determines the magnitude and rate of degradation of the rebar **/13/**. The building regulations for fire safety recommend that the minimum periods of the fire resistance for buildings should be of 90 min. These fire tests results show that concrete beams reinforced with Glass Fibre Reinforced Polymer (GFRP) rebar will meet the fire design requirements for the minimum periods of fire resistance (fire endurance) for the load. A minimum clear concrete cover of 70 mm is recommended for design of GFRP-RC beams rebars under fire conditions **/14/**.

Features and benefits of FRP rebars

- *Non-Corrosive* - do not corrode in wide variety of corrosive environments including chloride ions.
- *High Strength-to-Weight Ratio* - provides good reinforcement in weight sensitive applications.
- *Non-Conductive* - provide excellent electrical and thermal insulation.
- *Excellent Fatigue Resistance* - performs very well in cyclic loading situations.
- *Good Impact Resistance* - resists sudden and severe point loading.
- *Magnetic Transparency* - not affected by electromagnetic fields; excellent for use in MRI and other types of electronic testing facilities.

- *Lightweight*_- easily transported in the field without need for expensive heavy lifting equipment.

3.0 DEGRADATION OF CONCRETE STRUCTURES

The degradation of concrete structures can be divided into two stages, the initiation period and the propagation period. The initiation period is defined as the time from exposure until chlorides have penetrated the concrete cover and reached a critical concentration to start corrosion. The propagation period is considered to be the time from which the reinforcing steel starts to corrode until a critical limit of a material property (such as mechanical strength) has been reached.

3.1 Corrosion of Rebars in Concrete:

Concrete normally provides reinforcing steel with excellent corrosion protection. The high alkaline environment in concrete results in the formation of a tightly adhering film, which passivates the steel and protects it from corrosion. Corrosion of steel, however, can occur if the concrete is not of adequate quality. Chloride ions are the major cause of premature corrosion of steel reinforcement. Carbonation also cause corrosion by reducing alkalinity of the concrete. The rate of corrosion of steel reinforcement embedded in concrete is strongly influenced by environmental factors. Other factors that affect the rate of corrosion are heterogeneities in the concrete and the steel, pH of the concrete, pore water, carbonation of the Portland cement paste, cracks in the concrete, stray currents, design features, mix proportions and depth of cover over the steel. Fig. 4 shows the deterioration of concrete due to corrosion occurs because the products of corrosion (rust) occupy a greater volume than the steel and exert substantial stresses on the surrounding concrete **/15/.** The outward manifestations of the rusting include staining, cracking and spalling of the concrete resulting in reduction of cross-section of the steel.

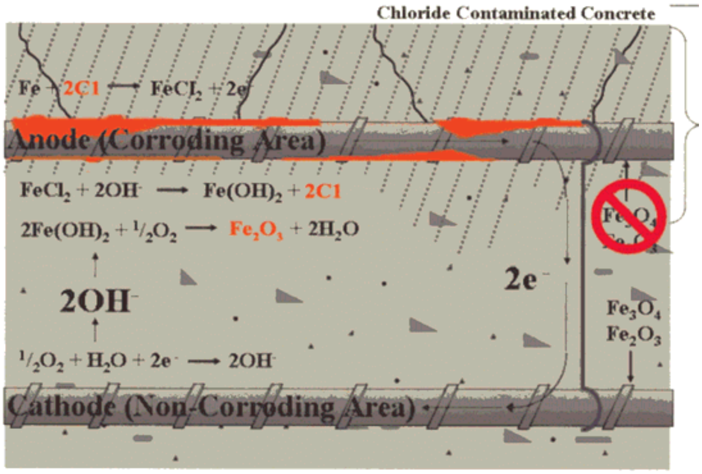

Fig. 4: Corrosion cell in concrete

3.1.1 Mechanism of corrosion of steel in concrete:

Exposed steel will corrode in moist atmospheres due to differences in the electrochemical potential on the steel surface by the formation of anodic and cathodic sites. The metal oxidises at the anode where corrosion occurs **/16/.**

Fe (metal) --> Fe^{2+} (aq.) + $2e^-$ (1)

Simultaneously, reduction occurs at cathodic sites, typical cathodic processes being:

$O_2 + 2H_20 + 4e^-$(metal) --> $4OH^-$(aq.) (2)

$Fe^{2+} + 2OH^-$ --> $Fe(OH)_2$ white corrosion product (3)

$Fe(OH)_2 + 2H_2O + O_2$ --> $4Fe(OH)_3$ Red Rust (4)

3 Fe + 8 OH^- --> $Fe_3O_4 + 4H_2O$ + 8 e^- Black Rust (5)

At high chloride concentrations:

Fe + $2Cl^-$ --> $FeCl_2$ --> $Fe^{++} + 2Cl^-$ + 2 e^- Yellowish green (6)

$$O_2 + 2H_2O + 4e^- \text{-->} 4OH^- \quad (7)$$

$$6FeCl_2 + O_2 + 6H_2O \text{-->} 2Fe_3O_4 + 12H^+ + 12\ Cl^- \quad (8)$$

The products of (1) & (2) reactions combine together and in the last stage they produce a stable film that passivates the reinforcing steel. The stability of this film depends essentially on the oxygen availability that controls the reaction and on the pH of the interstitial solution in the interface steel/concrete. The passive film is provided by the presence of a $Ca(OH)_2^-$ rich layer that adheres to the steel, hindering the cathodic reaction. In the presence of chlorides, the passive film is locally destroyed and a process of localised corrosion is then initiated. Harmful chlorides must reach the steel in the form of Cl^-. Concrete, however, has the capacity to bind the chloride ions leading to the formation of calcium chloroaluminate (Friedel's salt), a complex between the hydration products of cement and chloride: $[Ca_2Al(OH)_6]Cl \cdot 2H_2O$ or $C_3ACaCl_2 \cdot 10H_2O$, where C_3A denotes tricalcium aluminate. These salts partly immobilise chlorides and consequently determine the chloride level required to initiate the corrosion process. Friedel's salt is formed due to the adsorption of the bulk Cl^- present in the pore solution into the interlayers of the principal layer $[Ca_2Al(OH^-)_6 \cdot 2H_2O]^+$ of the aluminoferrite structure to balance the charge. Associated with this process, a cation (usually that associated with Cl^-) is also removed from solution to maintain ionic charge neutrality and binds with the calcium–silicate–hydrate (C–S–H) lattice. The microstructure of chloroaluminates plays an important role in the process of chloride fixation **/17/.** The factors responsible for corrosion of steels exposed to chlorides are shown in Fig. 5. Fly ash reacts with lime to form stable calcium silicate and aluminate hydrates. The hydrates fill the voids in concrete, removing some of the lime and thus reducing chloride permeability, which improves the chloride resistance of fly ash blended concrete /**4**/.

3.1.2 Chloride ingress:

Capillary absorption, hydrostatic pressure and diffusion are the means by which chloride ions can penetrate concrete. The most familiar method is diffusion, the movement of chloride ions under a concentration gradient. For this to occur, the concrete must have a continuous liquid phase and there must be a chloride ion concentration gradient. A second mechanism for chloride ingress is permeation, driven by pressure gradients. A more common transport method is absorption. As the concrete surface is exposed to the environment, it will undergo wetting and drying cycles. When water (possibly containing chlorides) encounters a dry surface, it will be drawn into the pore structure through capillary suction. Absorption is driven by moisture gradients. Of the three transport mechanisms described above that can bring chlorides into the concrete to the level of the rebar is diffusion. In the bulk of the concrete, the pores remain saturated and chloride ion movement is controlled by concentration gradients. The presence of chlorides at the steel surface in concentration higher than the critical threshold is generally considered in the range of 0.4–1% by cement weight /**18**/.

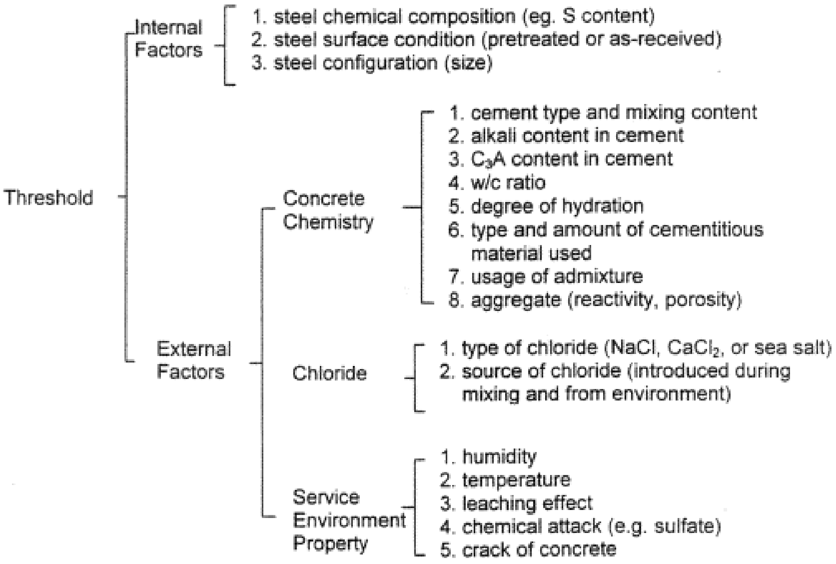

Fig. 5: Potential influences on the corrosion threshold for steels exposed to chlorides.

3.1.3 Chloride-induced corrosion of steel:

The electrochemical process of corrosion of the reinforcing bar embedded in concrete consists of anodic and cathodic reactions. As discussed above, the anodic reaction cannot occur until the passive iron oxide film is permeated by the Cl^- ions. The cathodic reaction cannot occur until a sufficient supply of oxygen and moisture are available at the steel surface. The anodic and cathodic reactions must balance each other; if either is limited, the corrosion process as a whole is limited. The corrosion of reinforcing steel by chloride ions depends on several factors, including chloride concentration, cement type, chloride penetration rate, oxygen level, concrete resistivity and temperature. Chloride concentration in concrete plays a major role in destroying the passivity of reinforcing steel. There are two sources of chlorides: internal chlorides present in the concrete mix and external chlorides from the sources such as sea water, brackish ground water and soils that diffuse through the cured concrete section. However, not all of these chlorides are responsible for corrosion. Only the water soluble chlorides present in the pore solution are responsible. The water soluble chlorides are not uniformly distributed along reinforcing steel; this nonuniform distribution may lead to the development of a corrosion cell. The threshold value of chloride ions necessary to initiate corrosion of reinforcing steel depends on the level of hydroxyl ions in the pore solution, which is reduced by leaching, carbonation or magnesium sulfate attack. pH level reduces the threshold value of chloride ions to initiate corrosion. The depassivation of reinforcing steel is a function of the Cl^-/OH^- ratio in the pore solution rather than that of chloride content alone. Cl^-/OH^- ratio of 0.3 has been to be the critical ratio below which reinforcing steel is not susceptible to chloride-induced corrosion **/19/.**

3.1.4 Theoretical background of chloride diffusion prediction

Chloride ion diffusion into the micropores of concrete can be modeled to predict chloride concentration at the reinforcing bar surface in concrete. Fick’s second law of diffusion is frequently used for this purpose where chloride ion diffusion into concrete is from one direction only. This enables prediction of the apparent chloride diffusion coefficient of concrete when the chloride concentration at any time is defined as a function of depth as

$$\delta C / \delta t = D\, \delta^2 C / \delta x^2 \tag{9}$$

An analytical solution to the above equation was proposed by Browne, assuming that the flux of chlorides at any time is proportional to the chloride concentration gradient in the concrete of a semi-infinite medium.

$$C_x = C_s[1 - \mathrm{erf}(x/2(D_a t)^{1/2})] \qquad (10)$$

where C_x is the chloride ion concentration at depth x after exposure time t for a surface chloride concentration of C_s at the concrete surface, D_a is the apparent chloride diffusion coefficient and the expression erf is the Gaussian error function. The Gaussian error function can be defined by the expression given below **/20/**:

$$\mathrm{erf}(z) = 2/(\pi)^{0.5}\, e^{-t} \qquad (11)$$

Corrosion does not commence unless the chloride content at the rebar surface in the concrete exceeds a critical value known as the threshold chloride level. Many factors affect the threshold level including concrete mix proportions, environmental conditions, the type of cement, mineral additives, etc. It has been reported that a relatively lower chloride concentration may be sufficient to initiate rebar corrosion in concrete exposed in the splash zone of a marine environment than concrete in the submerged zone. Considering exposure conditions frequently encountered, several researchers have attempted to assess the threshold chloride content for uncracked normal-strength concrete and have reported that the threshold chloride content may vary from 0.2% to 0.5% by weight of cement. Chlorides in concrete can be found in different forms. Some of the chlorides are chemically bound to cement paste to form calcium chloroaluminates and calcium chloroferrite; some are physically absorbed to the pore wall and some are free chlorides dissolved in the pore solution. In concrete, only chlorides dissolved in pore water cause corrosion, not those chemically bound in the cement phases.

3.1.4.1 Effect of curing on chloride diffusion:

The chloride concentration decreases with the depth and the period of curing. A minimum of 80% humidity is required for cement hydration. If concrete is not sufficiently cured, the permeability of the surface layer may be increased by 5 to 10 times. High wind and temperatures encourage drying of the concrete surface, leading to insufficient curing. The sensitivity of curing is especially pronounced if cements with high percentages of supplementary cementing materials (e.g. blast furnace slag, fly ash **/4/**, or silica fume) are used. Table 4 shows the coefficient of chloride diffusion in the concrete cured for varying durations. A significant reduction in the co-efficient of concrete diffusion was noted in concrete specimens cured for 28 days as compared to other curing periods.

3.1.4.2 Effect of W/C ratio on chloride diffusion:

The chloride concentration generally decreased with a decrease in the water/cement ratio. Concrete prepared with a high water/cement ratio and C_3S/C_2S ratio will have a more open and continuously linked pore structure with lower density and higher permeability, although such a concrete would still easily meet the 28-day compressive strength requirement. Therefore, concrete specifications for reinforced concrete structures in aggressive exposure conditions should be based on the W/C ratio rather than the strength. The data on coefficient of chloride diffusion is shown in Table 5 **/21/**.

Table 4

Effect of curing period on chloride diffusion **/21/.**

S.No	**Curing Period (Days)**	**Chloride Diffusion Coefficient (Cm^2/S)**
1	1	2.39×10^{-10}
2	3	2.25×10^{-10}
3	14	2.15×10^{-10}
4	28	0.07×10^{-10}

Table 5

Effect of water/cement ratio on chloride concentration **/21/.**

S.No	**Water/Cement Ratio**	**Chloride Diffusion Coefficient (Cm^2/S)**
1	0.40	1.18×10^{-10}
2	0.50	5.95×10^{-10}
3	0.65	6.92×10^{-10}

3.1.4.3 Effect of admixtures on chloride diffusion:

Concrete specimens modified by the addition of an epoxy showed that the lowest chloride concentration while those modified with an acrylic admixture showed the maximum chloride concentration. The co-efficient of chloride diffusion for the concrete specimens of this series are summarized in Table 6.

Table 6

Effect of concrete modification on chloride diffusion.

S.No	Concrete Modification Type	Chloride Diffusion Coefficient (Cm^2/S)
1	Acrylic	$2.700 X 10^{-10}$
2	Latex	$1.160 X 10^{-10}$
3	Epoxy	$0.670 X 10^{-10}$

3.1.4.4 Effect of cement content on chloride diffusion:

The presence of sufficient cement produces a cohesive mix that produces a dense concrete thereby producing fewer pores. The data on chloride diffusion coefficients in the concrete specimens prepared with cement content of 270, 390 and 450 kg/m^3 are summarized in Table 7. While there was no significant change in the chloride diffusion co-efficient in the concrete specimens prepared with cement contents of 270 and 390 kg/m^3 the decrease in the chloride diffusion co-efficient was almost one fold in the concrete specimens prepared with a cement content of 450 kg/m^3. These data also emphasize the usage of high cement content to produce a durable concrete.

Table 7

Effect of cement content on chloride diffusion

S.No	Cement Content (Kg/M^3)	Chloride Diffusion Coefficient (Cm^2/S)
1	270	$4.139 X 10^{-10}$
2	390	$8.950 X 10^{-10}$
3	450	$0.300 X 10^{-10}$

3.1.5 Properties of the Concrete that Affect the Chloride Penetration Rate

The rate of ingress of chlorides into concrete depends on the pore structure of the concrete, which is affected by factors including materials, construction practices and age. The penetrability of concrete is obviously related to the pore structure of the cement paste matrix. This will be influenced by the water-cement ratio of the concrete, the inclusion of supplementary cementing materials, which serve to subdivide the pore structure and the degree of hydration of the concrete. Pa Pa Win *et al* found that the reinforced concrete specimens having cracks showed rapid penetration of Cl− ion, which finally reached the steel and penetration along the steel also occurred /**22**/. Specimens with low w/c ratio of 0.25 showed lower concentration profile and penetration depth both from exposed surface and around the crack compared with w/c ratios of 0.45 and 0.65. No penetration along the steel was observed for specimens with w/c of 0.25. The increase in w/c led to a higher ingression rate of Cl− ions, not only from the exposed surface, but also around the crack. It was found from Fig. 6 that the movement of Cl− ions along with the bulk solution through the crack and within the concrete can occur when the capillary suction is taking place. This fact has great influence, rather than diffusion mechanism, and should not be ignored for real structures. There might have been a critical limit of free ion movement due to flow of bulk solution, followed by diffusion mechanism after the steady stage of moisture flow.

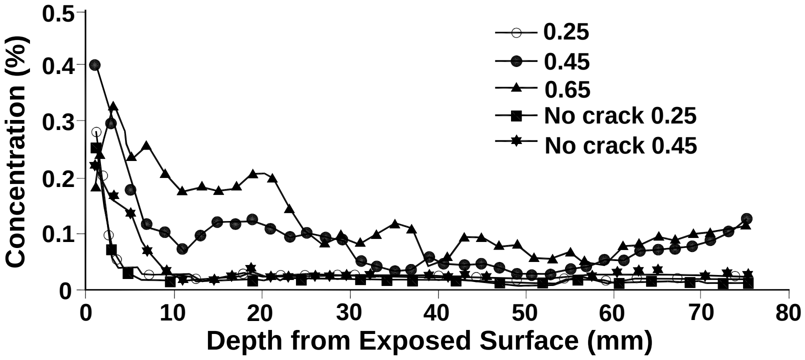

Fig. 6: Cl− ion concentration profile of w/c series.

3.2 Ageing of Concrete:

3.2.1 Alkali aggregate reaction:

Alkali aggregate reaction (AAR) is a chemical reaction where sodium and potassium ions in solution react with certain types of aggregate in the concrete. The reaction forms a hygroscopic alkali-silica gel which imbibes water and swells. The swelling forces generated may be sufficient to disrupt aggregate and the surrounding concrete, causing expansion, cracking and associated deterioration. AAR depends on the availability of three factors, viz alkalis liberated from cement during hydration, siliceous minerals present in certain kinds of aggregates and water. The alkali-silica reaction is the reaction of silica-rich aggregates with alkaline solution in the micropores of concrete and is one of the main chemical reactions causing severe deterioration of concrete. The reaction involved:

$$4SiO_2 + 2NaOH = Na_2Si_4O_9 + H_2O \quad (12)$$

$$SiO_2 + 2NaOH = Na_2SiO_3 + H_2O \quad (13)$$

However, the chemical composition of alkali –silica gel is variable and indefinite. Vivian **/23/** indicated that it is the OH^- ion concentration is important to this reaction. Chemical mechanism of the reaction is followed by two-process **/24/**:

a) Acid-base reaction

$$H_{0.38}SiO_{2.19} + 0.38NaOH = Na_{0.38}SiO_{2.19} + 0.38H_2O \quad (14)$$

b) Attack of the siloxane bridges and disintegration of the silica

$$H_{0.38}SiO_{2.19} + 1.62NaOH = 2Na^{2+} + H_2SiO_4^{2-} \quad (15)$$

The first stage involves hydrolysis of the reactive silica by OH^- to form an alkali-silica gel, the later stage being the absorption of water by the gel, which will increase the volume. Cracks thus provide access to the interior of the concrete and allow other degradation mechanisms to operate.

3.2.1.1 The alkali requirement in alkali-silica reaction:

3.2.1.1.1 The sources of alkali can be from

- Portland cement
- Supplementary cementing materials (e.g., fly ash, slag, silica fume)
- Aggregates

- Chemical admixtures.
- External sources (e.g., seawater and deicing salts)
- Wash water

Of the above materials, Portland cement is the main contributor of alkalis. The alkalis present in Portland cement are in the form of potassium oxide (K_2O) and sodium oxide (Na_2O). The quantity of alkalis in Portland cement is

$$Na_2O_e = Na_2O + 0.658K_2O \quad (16)$$

where: Na_2O_e = Total sodium oxide equivalent (or equivalent soda), in percent by mass
Na_2O = sodium oxide content, in percent
K_2O = potassium oxide content, in percent

Hawkins **/25/** recommended that the alkali content of the cement should be below 0.6% by weight and that the mass of alkalis from all sources should be kept below 3.0 kg/m^3 in the concrete for minimising the risk of damage to concrete by alkali-aggregate reaction.

3.2.1.2 The reactive silica component in the aggregate:

The term reactive refers to aggregates that tend to break down under exposure to the highly alkaline pore solution in concrete and subsequently react with the alkali-hydroxides (sodium and potassium) to form alkali silica reaction (ASR) gel. The inherent reactivity of aggregates depends on several factors, including aggregate mineralogy, degree of crystallinity and solubility (of the silica in pore solution). The rocks and minerals shown in Table 8 represent the rocks and minerals that are most prone to ASR.

Table 8

Rock Types and Reactive Minerals Susceptible to ASR

Rocks	Reactive minerals
Arenite	Crisobalite
Argillite	Cryptocrystalline (or microcrystalline) quartz opal
Arkose	Strained quartz tridymite
Chert	Volcanic glass

3.2.1.3 The role of moisture in alkali-silica reactivity:

Alkali-silica reactivity requires water to proceed. Water has a dual role, firstly, it is essential as the carrier of alkali cations and hydroxyl ions and secondly, it is absorbed by the hydroscopic gel which swells, developing pressures sufficient to crack the concrete. Below 70% relative humidity (RH) expansion and expansive reaction are negligible, but above 80% RH, the expansive effects are increased dramatically. Data supporting the importance of moisture on expansion are shown in Figure 7, where different reactive aggregates were stored under different moisture conditions, and the expansion of concrete prisms was assessed by ASTM C 1293 /**25**/

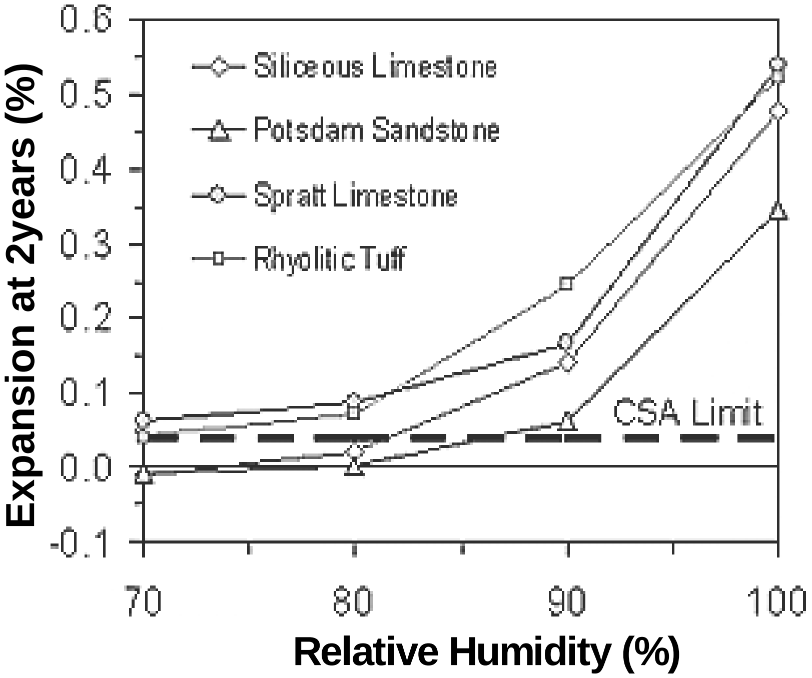

Fig. 7: Effect of relative humidity on expansion using ASTM C 1293.

3.2.1.4 Microstructural observation of ASR:

Figure 8 shows a thin-section cut from concrete affected by ASR, which is viewed under transmitted-light microscopy. The reaction product of ASR gel is seen, as is a crack forming through the aggregate and extending into the surrounding cement paste. The crack itself also is filled with ASR gel in some locations. This type of damage is typical of ASR-induced deterioration at the microstructural level of concrete.

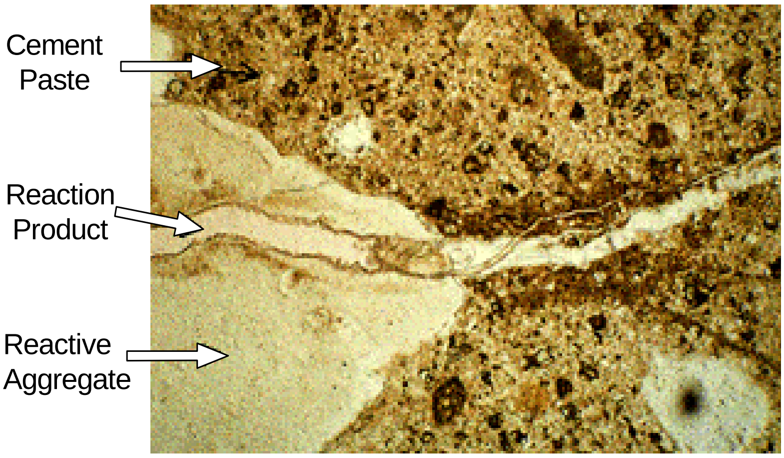

Fig. 8: Thin-section cut of ASR-damaged concrete, showing ASR gel and typical crack pattern (through aggregate and into surrounding matrix).

3.2.1.5 Minimizing or Preventing ASR in New Concrete:

The most common methods of minimizing the risk of expansion due to ASR include:

- Using nonreactive aggregates.
- Limiting the alkali content of concrete.
- Using supplementary cementing materials (SCM) includes fly ash, ground- granulated blast furnace slag, silica fume and combinations of SCMs (ternary blends).
- Using lithium compounds like lithium nitrate ($LiNO_3$) which alters the ASR product composition, resulting in a less expansive product.

3.2.1.6 Mitigating ASR in Existing Concrete:

When ASR-induced expansion and damage already has manifested itself in a field structure, there are some available techniques that can help extend the service life of the structure, as described in detail in CSA A684-00. To minimize future damage to such structures:

- Provide adequate or improved drainage (to minimize availability of

moisture).
- Apply claddings or coatings to further limit moisture ingress.
- Treat existing cracks to minimize future expansion (and direct moisture ingress, deicing salts, etc.).
- Avoid future use of deicing salts that will increase alkali content within the structure.
- Restrain or confine expansion of structural element.
- Chemically suppress ASR using lithium compounds.

A test was recently developed for identifying alkali–silica reaction products in concrete. Staining concrete with uranyl ions, which have a characteristic greenish yellow fluorescence under short wave ultraviolet light, identifies the reaction products. This staining technique appears to uniquely identify the products of alkali–silica reaction. Thus, this technique can detect the alkali–silica reaction taking place before any concrete expansion and cracking occurs. Ultrasonic pulse velocity and attenuation measurements have been found sensitive to concrete expansion and cracking caused by alkali–silica reaction.

The following ASTM tests identify reactive aggregates:
- ASTM Practice for Petrographic Examination of Aggregates for Concrete (C 295)
- ASTM Test for Potential Reactivity of Aggregates (C 289), which is a rapid chemical test
- ASTM Test for Potential Alkali Reactivity of Cement–Aggregate Combinations (C 227), which consists of a mortar bar expansion test
- C 1260-05 Standard Test Method for Potential Alkali Reactivity of Aggregates (Mortar-Bar Method)
- ASTM C441: Standard Test Method for Effectiveness of Mineral Admixtures or Ground Blast Furnace Slag in Preventing Excessive Expansion of Concrete Due to the Alkali-Silica Reaction
- ASTM C 856: Practice for Petrographic Analysis of Hardened Concrete
- ASTM C 1293: Standard Test Method for Concrete Aggregates by Determination of Length Change of Concrete Due to Alkali-Silica Reaction

3.2.2 Carbonation of concrete structures:

One of the main causes of reinforced concrete corrosion is the carbonation of concrete. Carbonation refers to a reaction between the calcium hydroxide in the cement paste and carbon dioxide in the environment, which, in the presence of moisture, results in a reduction of the concrete pH /**26**/. The reaction produces calcium carbonate, which is a neutral product. The main consequence of carbonation is the drop in the pH of the pore solution in the concrete from the standard values between 12.5 and 13.5 to a value below 9 in the fully carbonated zones resulting in breakdown of the passive layer which protects the reinforcing steel from corrosion. The depth of carbonation may be determined by phenolphthalein test of a removed core sample. The basic factor influencing carbonation is the diffusivity of the hardened cement paste. Carbonation rate is controlled by the ingress of CO_2 into concrete pore system by diffusion with a concentration gradient of CO_2 acting as the driving force. Factors affecting diffusion rate include the type and amount of cement, porosity of the material, time of curing, type and quantity of pozzolanic additions /**27**/.

3.2.2.1 Reactions of CO_2:

During hydration, the anhydrous calcium oxide of the cement, CaO, forms calcium silicate hydrate, $mCaO{\cdot}SiO_2{\cdot}nH_2O$, denoted by C-S-H, and calcium hydroxide, $Ca(OH)_2$. Whereas C-S-H is insoluble, the alkaline $Ca(OH)_2$ may dissolve in the pore liquid. Additional alkalis are supplied in form of sodium and potassium oxides of the cement. They dissolve in the pore liquid during hydration, forming sodium, potassium and hydroxyl ions, respectively. As these ions do not take part in the formation of the major cement hydration products, they accumulate in the pore solution and thus render calcium very insoluble. The pH of such pore fluids may well be greater than 12.4. The CO_2 that penetrates into concrete reacts with the alkaline hydration products of the cement paste. The reaction is called carbonation. The reaction kinetics of carbonation is a two- stage process **/28/.** In the first stage, CO_2 diffuses from the atmosphere into the partially dried capillary pores and combines with water to form carbonic acid:

$$CO_2 + H_2O \longrightarrow H_2CO_3 \qquad (17)$$

Then, calcium hydroxide $Ca(OH)_2$ (also known as portlandite) dissolves in the pore water and reacts with dissolved CO_2 to form calcium carbonate (calcite)

$$Ca(OH)_2(aq) + H_2CO_3 \xrightarrow{H_2O} CaCO_3(aq) + 2H_2O \qquad (18)$$

The produced $CaCO_3$ precipitates very quickly to the solid matrix. To some extent, C-S-H also reacts with CO_2; however, this reaction is difficult to figure out in detail because of the variety of C-S-H phases. Exact stoichiometric relations are unknown. The formation of crystalline calcium carbonate and amorphous hydrous silica can be simply described as follows /**29**/:

$$\text{C-S-H} + CO_2(aq) \xrightarrow{H_2O} CaCO_3(aq) + SiO_2 \,.\, nH_2O \qquad (19)$$

After hydration, sodium hydroxide and potassium hydroxide are completely dissolved in the pore liquid and therefore react readily with penetrating CO_2 that dissolves in the pore liquid. After neutralization of the alkali ions in form of carbonates, $Ca(OH)_2$ dissolves in the pore solution to restore the chemical equilibrium. As long as calcium ions are available, the formed sodium and potassium carbonates are unstable and reorganize with the dissolved $Ca(OH)_2$ to calcium carbonate, which crystallizes into stable calcite and metastable aragonit. The calcium carbonate is almost insoluble. Both dissolution of alkalis and solution of CO_2 require free water in the pores. Only when the soluble $Ca(OH)_2$ is completely bound in $CaCO_3$ are the sodium and potassium carbonates stable. Due to the concentration of soluble $Ca(OH)_2$ in the cement paste being far greater than those of sodium hydroxide and potassium hydroxide, it is the governing factor for the alkalinity of the pore liquid. During carbonation of $Ca(OH)_2$, a volume increase of 11% for calcite and 3% for aragonite formation was reported by De Ceukelaire and Van Nieuwenburg **/30/**. A recent study by Dias **/31/** measures a decrease in total porosity and pore volume of ordinary Portland cement concrete during carbonation resulting in denser concrete.

3.2.2.2 Temperature effect on CO_2 diffusion:

Increasing temperature decreases, the solubility of CO_2 and also acid formation since diffusivity of CO_2 is increased due to increased activity energy. The temperature dependence on diffusion follows Arrhenius's Law.

It is shown that activity energy of CO_2 is almost constant in certain temperature ranges (20 ~ 40 °C) regardless of W / C ratios of concrete. The temperature effect on diffusivity of CO_2 is given as,

$$D(T) = D_{ref}.\exp[U/R(1/T_{ref} - 1/T)] \tag{20}$$

where D_{ref} is reference diffusivity (the same as $D_{CO2}{}^{eq}$ in cracked concrete and D_{CO2} in sound concrete), U (8500 Cal/mol K) is activity energy of CO_2 and T_{ref} (298 K) is reference temperature.

3.2.2.3 Porosity change effect on CO_2 diffusion:

In general, the diffusivity coefficient of CO_2 is obtained by experiments with N_2 or O_2 multiplied by the molecular mass ratio of CO_2. The diffusivity coefficient is changed by porosity change due to carbonation process. It is well known that during carbonation dissolved CO_2 reacts with hydrates and forms $CaCO_3$ and the volume of hydrates is increased **/32/.** It is also reported that the reduction in pore volume observed for the cement matrices could be associated with the deposition of $CaCO_3$ formed during carbonation. The volume of the $CaCO_3$ formed exceeds that of the hydrates, thus causing a reduction in porosity **/33/.** Change in porosity is reported to be more decreased in concrete with relatively lower W / C ratio **/34-35/.** Carbonation has a clear influence on porosity and this decrease is more important for higher W / C ratios. Fig. 9 shows that, with increase in crack width and W/C ratio, the diffusion coefficient D $CO_2{}^{eq}$ / D CO_2 also increases proportionately **/36/.**

3.2.2.4 Effect of carbonation and chloride attack:

Carbonation of concrete followed by chloride attack accelerates the corrosion rate and its intensity in comparison with the converse sequence of the action of both media /**37**/. Fig. 10 shows that the maximal value of material loss was reached by the combination of carbonation and penetration by NaCl solution. This intensifying effect of the primary carbonation followed by chloride attack is evidently a consequence of the decreased alkalinity of pore solution in concrete and resulted in electrochemically active status of reinforcement becoming more vulnerable to the chloride attack

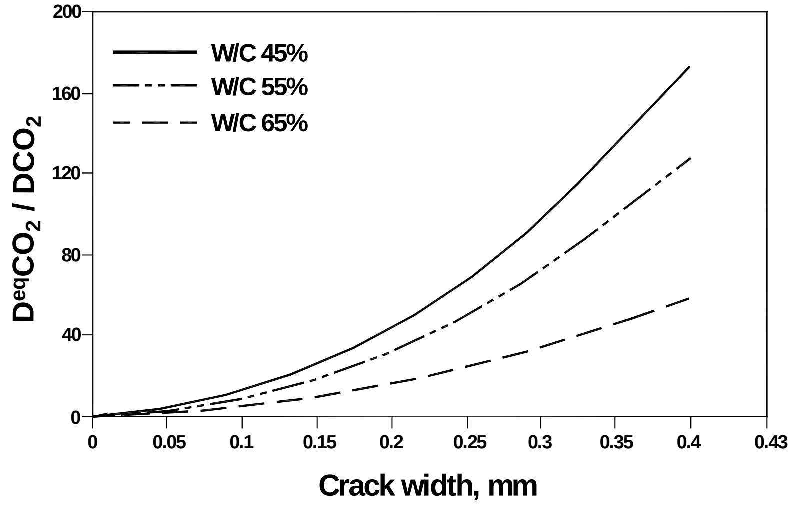

Fig. 9: Ratio of D_{CO2}^{eq} / D_{CO2} Vs. crack width for various W / C ratios.

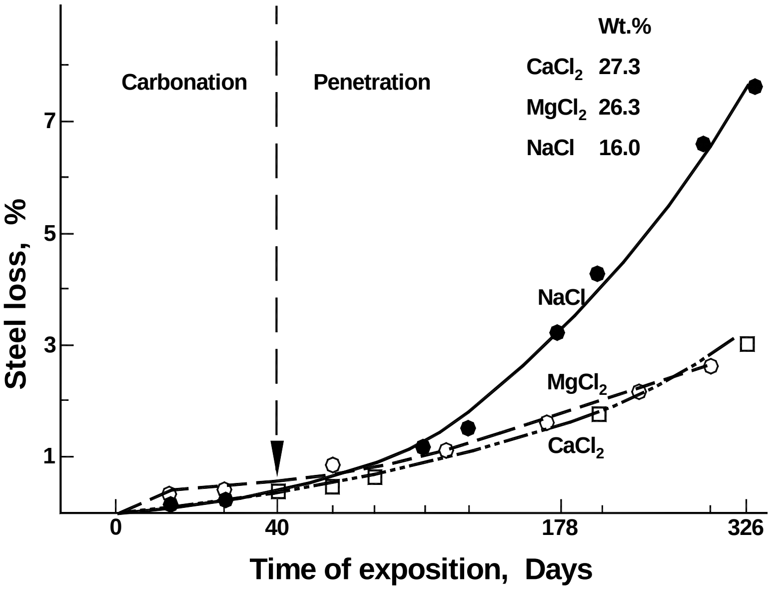

Fig.10: Material loss due to corrosion of specimens exposed to carbonation and Subsequently penetrated by chloride solution.

3.2.3 Influence of sulphate attack on concrete:

Solid salts do not attack concrete, but when present in solution they can react with hardened cement paste. Sulphates are present in sea water and industrial effluents. Sulphate found in groundwater (and also in soil and sea water) can chemically interact with the constituents of hydrated cement paste and cause degradation of the concrete. This is known as sulphate attack. Sulphate attack is known to cause two distinctly different types of concrete degradation: concrete cracking by expansive chemical products and progressive loss of concrete strength after prolonged exposure. Mechanisms and degree of sulphate reaction depends on the following parameters:

a) Concentration of sulphate ions.
b) Cations present in the sulphate solution (i.e., sodium, potassium, ammonium or magnesium)
c) C_3A content of cement
d) Density and permeability of the concrete

Sulphates in the groundwater chemically react with calcium sulfoaluminate, also called the tricalcium aluminate phase, which is a constituent of hydrated cement paste. This reaction produces an expansive high-sulphate chemical product called ettringite, which causes concrete cracking after short-term exposure. The extent of damage to the exposed concrete depends on the sulfate content of the groundwater and on permeability and composition of the concrete. Groundwater with a low concentration of sulphate ions can produce solutions of high concentration if it wets the concrete surface, evaporates and builds up a quantity of precipitated salts that then dissolve to form a nearly saturated solution that could cause concrete cracking in the long term.

Sulphate converts calcium hydroxide into a large volume of calcium sulphate (gypsum)

$$Ca(OH)_2 + Na_2SO_4.10H_2O \longrightarrow CaSO_4.2H_2O + 2NaOH + 8H_2O \qquad (21)$$

The second hydration product, tricalcium aluminate hydrate, reacts with sulphate solution to form sulphoaluminate hydrate, which has a greater volume than that of the original compound.

$$2(3CaO.Al_2O_3.12H_2O)+3(Na_2SO_4.10H_2O) \longrightarrow 3CaO.Al_2O_3.3CaSO_4.31H_2O + 2Al(OH)_3 + 6NaOH + 17\ H_2O \quad (22)$$

Calcium sulphate attacks only calcium aluminate hydrate, forming calcium sulphoaluminate. Magnesium sulphate attacks calcium silicate hydrates as well as $Ca(OH)_2$ and calcium aluminate hydrate. In the early stages of penetration of sulphates and the chemical reaction, the products cause the concrete to gain strength as unoccupied pore spaces are filled. However, if enough of the reactants like tricalcium aluminate hydrate, sulphate and water are present in the concrete, the resultant internal expansive stress can be sufficient to cause deformation and cracking. The rate of sulphate attack increases with an increase in the concentration of the solution. A saturated solution of $MgSO_4$ leads to serious deterioration of concrete, which can be controlled by lowering W/C ratio. The concentration of the sulphate is of 1000 ppm is considered moderately severe and 2000 ppm are very severe. Concrete attacked by sulphate has a characteristic whitish appearance. The damage usually starts at edges and corners and is followed by progressive cracking and spalling. The vulnerability of concrete to sulphate attack can be reduced by the use of cement low in C_3A content and by partial replacement of pozzolans. The resistance of concrete to sulphate attack is tested in the laboratory by storing specimens in a solution of sodium or magnesium sulphate. Alternate wetting and drying accelerates the damage owing to the crystallization of salts in the pores of the concrete. The effect of exposure is estimated by the loss in strength of the specimen, by its expansion, by its loss of weight or by changes in its dynamic modulus of elasticity.

3.2.3.1 Effect of W/C ratio and cement content on the sulfate-resistance of concrete:

The effect of W/C ratio and cement content in the concrete mixes on sulfate attack resistance is evaluated in terms of the change in compressive strength. The strength increases with the increasing cement content and decreasing W/C ratio. Sulfate attack was more intense in the concrete specimens prepared with a high W/C ratio. However, as the cement content was increased to 390 kg/m^3, the strength gain was more predominant compared to the sulfate deterioration.

3.2.3.2 Effect of curing time on the sulfate-resistance of concrete:

Fig. 11 shows that the strength increases with the curing time **/20/**. Increased curing of a 0.45 W/C ratio mix results in a dense impermeable concrete which is not permeated by the sulfate bearing groundwater resulting in sulfate attack which is only confined to the concrete skin.

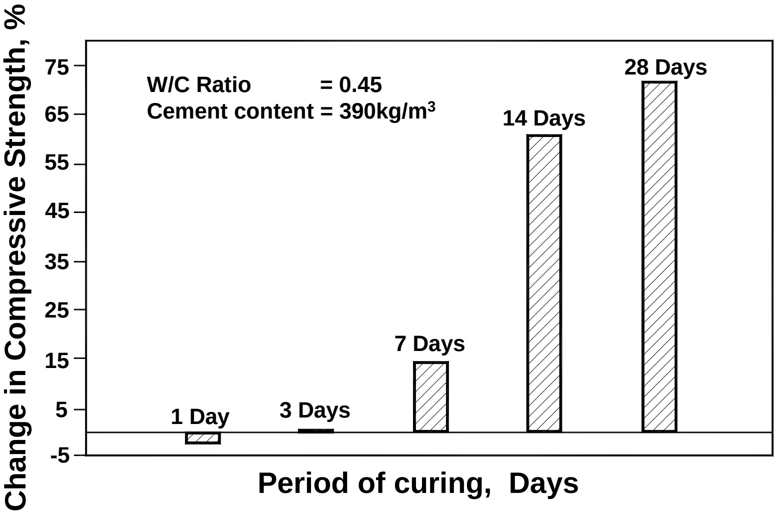

Fig. 11: Effect of curing period on change in compressive strength in buried concrete specimens.

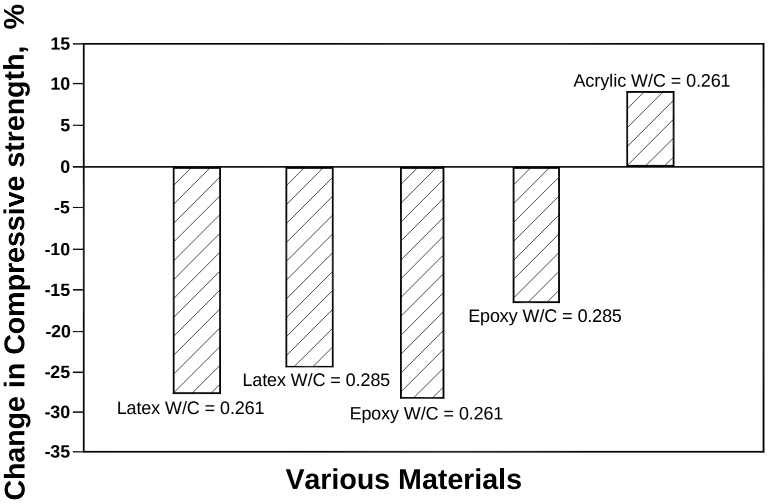

Fig. 12: Change in compressive strength of modified concrete specimens.

3.2.3.3 Effect of admixtures on the sulfate-resistance of concrete:

A reduction in strength was noted in latex and epoxy modified concrete specimens. This was because these admixtures polymerized more effectively in air than in water. Admixing concrete with latex and epoxy hinders the normal cement hydration. This behavior was not noted in the acrylic modified concrete specimens prepared with a water/cement ratio of 0.261 as shown in Fig. 12.

4.0 FACTORS AFFECTING CORROSION OF STEEL IN CONCRETE

The factors affecting corrosion of steel in concrete may be classified into two major categories:

4.1 External factors

1. ***Availability of oxygen and moisture at rebar level:***

The presence of moisture and oxygen supports corrosion. Moisture fulfills the electrolytic requirement of the corrosion cell and moisture and oxygen together help in the formation of more OH^- thereby producing more rust component, i.e., $Fe(OH)_2$.

2. ***Relative humidity and temperature:***

The relative humidity mainly affects the carbonation of concrete. In the range of 50–100% RH, the increase of environmental relative humidity decreases carbonation of concrete. However, Cahyadi and Uomoto /**38**/ found that, in the range of 30–50% RH, a decrease in environmental RH does not cause a decrease in carbonation of concrete especially in normal concentration of CO_2 even after a long period of exposure. A rise in temperature results in a two fold effect: (i) the electrochemical reaction rates are generally increased and (ii) the oxygen solubility is decreased resulting in a reduction in the rate of corrosion /**39**/. If the situation is conducive for corrosion to take place, the corrosion rate is increased by high temperature and high humidity. However, concrete deterioration due to low temperature results from a change in the water volume when water freezes. In larger capillary pores, freezing starts at 0^o C but in small pores, the temperature needs to be much lower before the water starts freezing.

3. ***Carbonation and entry of acidic gaseous pollutants to rebar level:***

The effect of carbonation and other acidic gases, such as SO_2 and NO_2, is due to their tendency to reduce the pH of the concrete. The fall in the pH to certain levels causes commencement of reinforcement corrosion.

4. ***Aggressive anions, mostly chloride ions, reaching to the rebar level, either through the concrete ingredients or from the external environment:***

Chloride (Cl^-) in concrete may be present in either of the following forms **/40/:**

'Acid soluble chloride' which is equal to the total amount of chloride present in the concrete or that is soluble in nitric acid.

'Bound chloride' which is the sum of chemically bound chloride with hydration products of the cement, such as the C_3A (tricalcium aluminate) or C_4AF (tetracalcium aluminoferrite) phases and loosely bound chloride with C–S–H gel, and

'Free or water-soluble chloride', which is the concentration of free chloride ions (Cl^-) within the pore solution of concrete and is extractable in water under defined conditions.

It is generally recognized that only the "free chloride" ions influence the corrosion process **/41/**. It is reported that the resistivity decreases and corrosion rate increases with an increase in the chloride content **/42/**. However, the change in pH is found to be insignificant due to a change in the chloride content of concrete.

4.2 Internal factors affecting reinforcement corrosion

Cement composition:

The cement in the concrete provides protection to the reinforcing steel against corrosion by maintaining a high pH in the order of 12.5–13 owing to the presence of $Ca(OH)_2$ and other alkaline materials in the hydration product of cement and by binding a significant amount of total chlorides as a result of chemical reaction with C_3A and C_4AF content of cement in concrete. Thus the threshold chloride value shifts to higher side with an increase in the C_3A content of cement **/43/**. The use of blended cement, such as microsilica-blended high-C_3A cement, is found to be concomitantly resistant to sulphate attack and chloride corrosion of reinforcement **/44/.**

Impurities in aggregates:

Aggregates containing chloride salts cause serious corrosion problems, particularly those associated with sea-water and those whose natural sites are in ground water containing high concentration of chloride ions.

Impurities in mixing and curing water:

Mixing and curing water, either contaminated with sufficient quantity of chloride or being highly acidified due to any undesirable substance present in water, may prove to be detrimental as for as corrosion of rebar is concerned.

Admixtures:

Addition of calcium chloride in concrete, as a common admixture for accelerating the hydration of cement is perhaps a most significant reason for the presence of chloride in concrete in the reinforced concrete (RC) structures exposed to normal weather conditions. Some water reducing admixtures also contain chlorides.

W/C ratio:

The W/C ratio, known to control principally strength, durability and impermeability of concrete, does not itself control the rate of corrosion of reinforcement. When RC structures are immersed in some aggressive solution, it is the ‘permeability’ of concrete, which is a function of W/C ratio, which affects the corrosion of rebar. The depth of penetration of chloride to a particular threshold value increases with an increase in the W/C ratio **/45/**. Carbonation depth linearly increases with an increase in the W/C ratio **/46/**. The oxygen diffusion coefficient also increases with increase in the W/C ratio **/47/**. Goto and Roy reported a 100-fold increase in the permeability of hardened cement paste when the W/C ratio was increased from 0.35 to 0.45 **/48/**. Al-Saadoun had observed that the time to initiation of reinforcement corrosion in a concrete with w/c ratio of 0.4 is 2.15 to 1.77 times more than that in concrete with a w/c ratio of 0.55, under the accelerated corrosion testing **/49/**. The permeability is significantly reduced for a W/C ratio below 0.45. From these discussions it is understood that the W/C ratio should be less than 0.45 and preferably around 0.40 to obtain good resistance against chloride diffusion. However, a low W/C ratio does not by itself assure concrete of low permeability. Thus, in addition to the low W/C ratio, the concrete must be properly proportioned and well consolidated to produce a concrete of low permeability.

Cement content:

The cement content in concrete does not only affect the strength but also has a significant effect on durability. Due to inadequate amount of cement in mix, the concrete is not consolidated properly leading to the formation of honeycombs and other surface defects. These honeycombs and surface defects help in the penetration and diffusion of corrosion causing agents, such as Cl^-, H_2O, O_2, CO_2, etc., in concrete. This results in the initiation of reinforcement corrosion due to the formation of differential cells. Further, concrete with low cement content has a lack of plastic consistency due to which it does not form a uniform passive layer on the surface of the steel bars. Therefore, it is important to maintain a minimum cement content from the durability point of view.

Aggregate size and grading:

Aggregate grading is another factor, which should be considered for high quality impermeable concrete. It has been observed that for a given W/C ratio, the coefficient of permeability of concrete increases considerably with increasing size of aggregates. Hence, the proportioning of coarse and fine aggregates is important for the production of a workable and impermeable concrete. The aggregate proportioning for this purpose consists of fixing the optimum volume fraction of sand in the total aggregate content. Maslehuddin observed that both ‘too much’ and ‘too less’ sand reduces the workability of concrete **/50/**. This enhanced workability on account of an optimum aggregate grading allows a reduction in the W/C ratio resulting in increased strength and durability of concrete.

Chemical composition and structure of the reinforcing steel:

The differences in the chemical composition and structure of reinforcing steel and presence of stresses in the reinforcement, either static or cyclic, create different potentials at different locations on the surface of reinforcement, causing the formation of differential corrosion cells, which leads to its corrosion.

5.0 CONTROL OF DETERIORATION AND CORROSION IN CONCRETE STRUCTURES

To control corrosion of reinforcing steel in concrete structures, the concrete must block the ability of ions that cause corrosion from making contact with the steel by retarding the progression of chloride diffusion. To do this, the following ways should be considered **/51/**:

- Reduce the permeability of the concrete
- Ensure at least 50 mm of concrete cover
- Coat the rebars with suitable protective coatings
- Use a corrosion inhibitor in the concrete
- Use cathodic protection
- Keep the concrete dry
- Use a pozzolan or, even better, a blended cement in the concrete
- Use a water-reducing agent
- Cure the concrete properly
- Use other special treatments

5.1Concrete:

5.1.1 Permeability

Corrosion occurs because a salt solution or water or carbon dioxide penetrates the concrete. Lowering the permeability of the concrete reduces the chances of contamination. The most critical aspect of controlling the permeability is the water-to-cement ratio. At a water-to-cement ratio of 0.5, carbonation will typically penetrate 3/8-inch in ten years. If the strength is low (3,000 psi or 20.7 mPa) carbonation can reach close to one inch in seven years. Strong concrete with a low water-to-cement ratio will have a low permeability and less susceptible to corrosion. A reduction of W/C ratio from say 0.7 to 0.3 lowers the coefficient of permeability by a factor of 100. As expected, porosity is observed to increase with W / C ratio. The relationship is obviously not linear. Porosity values range from 8% for the lowest W / C ratio of 0.3 to 13.5% for the highest W / C of 0.6. **/52/.**

Measurement of water permeability:

IS:3085-1965 gives the method of test for permeability of cement mortar and concrete **/53/**.

The coefficient of permeability is given by:

$$K = Q/(A*T*H/L) \tag{23}$$

Where

K = co-eff of permeability in cm/sec

Q = Quantity of water in millilitres percolating over the entire period of test after the steady state has been reached.

A = Area of the specimen face in sq.cm

T = Time in seconds over which Q is measured

H/L = Ratio of the pressure head to thickness of the specimen, both expressed in the same units.

Air and vapour permeability:

Permeability of concrete to air is of interest in structures such as nuclear containments and sewage tanks. Increasing the cement content of the mix (i.e., reducing W/C ratio) decreases the air permeability. The addition of flyash or pozzolana has a beneficial effect. Grading of aggregate is important to reduce air permeability of concrete. Prolonged curing reduces air permeability and rapid drying out increases air permeability through the development of fine shrinkage cracks. Water vapour transmission in concrete is reduced by an increase in the age of concrete, by a decrease in the W/C ratio and on prolonged moist curing. Vapour permeability decreases as the mean relative humidity increases.

5.1.2 Corrosion Inhibitor

Corrosion inhibitors used in concrete may be inorganic or organic or both. The inhibition mechanisms of these substances are still not very clear. It is believed that some inorganic-inhibiting compounds act as anodic inhibitors, by increasing the rate of formation of an oxide film barrier on the reinforcing steel surface. Some organic compounds inhibit corrosion by adsorbing onto the steel surface, preventing the breakdown of the passive film. Calcium nitrite is generally added as an admixture at about 2 percent (solids/cement) when the concrete is manufactured **/51/**. Calcium nitrite not only reduces the chances of corrosion in steel, but also increases the strength of the concrete. It also accelerates setting, which can be troublesome in summer. However, a retarder can be used with it to lengthen the time of setting without changing the corrosion-protection properties. The advantage of calcium nitrite is that it forms a protective film on the iron in concrete, blocking chloride ions from attacking. Since it is mixed throughout the concrete, it also prevents dissolved iron from moving away from the anode. This aids the build-up of reaction products on the rebars, preventing further corrosion /**51**/.

5.1.3 Concrete Moisture

For corrosion to occur, moisture must be present. Concrete placed inside an air-conditioned building will generally not be subjected to corrosion problems. Also, concrete that is kept saturated at 100 percent humidity at a constant temperature does not carbonate very readily or easily corrode. The worst condition is concrete that continually undergoes wetting and drying and temperature changes. Salt water moves into concrete quickly by capillary action when it is dry and carbon dioxide is also absorbed best when the humidity is low. Although totally dry concrete is an effective way to prevent corrosion, it is impractical in most cases.

5.1.4 A Water-Reducing Agent

Keeping the water-to-cement ratio low is one of the keys to making durable concrete with low permeability. Water-reducing agents help to make this easy since the same flow properties can be obtained with less water. High-range water-reducing agents are preferred towards better flow properties in lower W/C ratios. These materials may cost more initially, but they reduce the life-cycle cost of a concrete structure.

5.1.5 Concrete Curing

Precast concrete is usually better than ready-mixed concrete because of the more controlled curing that is done in a precast plant. Good curing allows the concrete near the surface to react more completely, which reduces the size of the pores and thus reduces the penetration of salt and carbon dioxide. Traditionally, curing has been a one-step process, but recently ACI Committee 308 has proposed that there are two periods of curing for which concrete must be protected /**51**/. Initial curing is the time between the disappearance of the bleed-water sheen and the end of the finishing process. However, some believe that waiting for the bleed water to disappear before starting the curing process will definitely produce cracked concrete. Final curing begins after finishing and continues until the required concrete properties have been achieved. This can be as short as three days for high-performance concrete or as long as six months for concrete with a high water-to-cement ratio (until no more gel space is available in the concrete). Curing should be started as soon as possible and continued as long as practical. An evaporation retarder, such as octadecanol, can be used when the concrete is still wet (before the bleed water disappears) and water can be gently sprayed on the concrete periodically after final set.

5.1.6 High performance concrete:

High performance concrete (HPC) definitely prevents corrosion in most environments. However, like normal concrete, it leaves several doubts over its performance when contaminated. It cannot help in the case where corroded bars are used for construction. Another problem in HPC is under cracked condition, HPC has more chances of corrosion at localised areas compared to normal concrete.

5.1.7 Coatings on Concrete surface:

A coating to concrete is intended to isolate external factors attacking the concrete. Basically, there are two types of coatings. These are pore block coatings and impregnable coatings. When to coat concrete is a question as it may affect the breathing of concrete. However, numerous organic and inorganic coatings have been developed for concrete surfaces. The various substances to coat concrete include bituminous coatings, linseed oil, chlorinated rubber, polyvinyl copolymers, acrylics, polyurethanes, epoxy resins etc. Aqueous solutions of sodium silicate, magnesium and zinc fluosilicates can react with the soluble calcium compounds and form insoluble calcium silicate or calcium fluosilicate. This treatment helps to increase surface hardness and reduce dusting. However, these treatments have been found to have only limited chemical resistance. Bituminous materials are made with either asphalt or coal tar and have excellent resistance to water and moisture. Coal tar pitches have excellent water resistance with moderate resistance to acids and alkalies. Acrylic latexes are resistant to heat, sunlight and weather. Polyvinyl acetate latex shows good resistance to chlorine and hydrogen sulphide gases. The styrene-butadine resins posses excellent resistance to both strong and weak acids as well as strong alkali, oil, grease and water. Exterior durability of these resins is good, but they tend to fade under sunlight. Two components epoxy resin films are extremely tough, hard and chemically resistant to most aggressive agents. Resistance to weathering is generally good. These coatings are also having good abrasion resistance. These coatings are often applied with a overcoat of self-polishing type of anti-fouling paints in order to discourage the attachment of bio-organisms from sea water. The most dangerous zone is the one within the splash area or partially immersed in sea water with respect to both corrosion of rebars and microbial attack of concrete structures. The best coating proposed for protecting in such severe and normal zones contain a primer coating made of silanes and siloxanes, followed by aliphatic acrylic paint coatings. These coatings increase the life to about 30 years in sea water. They have good resistance to UV radiation, chloride penetration and CO_2 absorption. There are also glass based coatings available in the market for such applications.

5.2 Control of Corrosion of Rebars:

Various methods are being used to extend the service life of reinforced concrete structures, which include coatings to concrete surface, coatings to the reinforcement, cathodic protection, chloride removal and corrosion inhibitors. Of the various methods to protect steel reinforcements, the use of corrosion inhibitors is found to be one of the effective methods to control rebar corrosion.

5.2.1 Inhibitors:

The use of inhibitors in concrete is an alternative option for preventing the corrosion of steel in concrete in the presence of chloride ions **/54/**. Inhibitors are substances which when added to an environment decrease the rate of attack on a metal. Corrosion inhibitors function by reinforcing the passive layer or by forming oxide layer and preventing outside agents from reacting with it. Corrosion inhibitors can be divided into three types: anodic, cathodic and mixed inhibitors, depending on whether they interfere with the corrosion preferentially at the anodic or cathodic sites or whether both are involved **/55/**. Anodic inhibitors decrease the rate of dissolution process by forming thin oxide layer and shielding the anodic sites. Cathodic inhibitors retard the cathodic reaction by acting on the cathodic sites and reduce the corrosion current. Earlier studies carried out on numerous inhibitors with most attention focused on sodium nitrite, potassium chromate, sodium molybdate and fluorophosphite. Calcium nitrite is the first corrosion inhibitor admixture commercialized on a large scale for reinforced concrete.

5.2.1.1 Calcium nitrite:

It inhibits corrosion by reacting with ferrous ions to form a protective ferric oxide film and Craig and Wood /**56**/ studied sodium nitrite, potassium chromate, and sodium benzoate using the polarization technique and found that sodium nitrite was the most effective corrosion inhibitor, but it had harmful effects on concrete strength. Similar results were also reported by Treadaway and Russel /**57**/ and found that sodium nitrite inhibited corrosion of steel bars in the presence of chlorides, whereas sodium benzoate did not. Rosenberg *et al.* studied the effect of calcium nitrite as an inhibitor in reinforced concrete /**58**/. They used polarization techniques for evaluation of the inhibitors and reported that the relative corrosion rates for samples soaked in saturated sodium chloride solution for 90 days with 2% and 4% admixed calcium nitrite were about a factor of 15 times lower than those without the calcium nitrite admixture. Berke /**59**/ reported that after 4 years of accelerated corrosion with chloride levels at the steel exceeding 7 kg/m^3 (12 lb/yd^2), the only uncorroded specimens were those which contained calcium nitrite. Berke and Sundberg /**60**/ showed that the use of calcium nitrite and micro silica significantly improved the durability of reinforced concrete in marine environment. Studies also showed that calcium nitrite, an anodic inhibitor, modifies the oxide film on the steel bar to be more protective than the film that naturally forms in concrete. The inhibitive action of calcium nitrite depends on its reaction with Fe^{2+} ions as follows /**61**/:

$$2Fe^{2+}+2OH^{-}+2NO_2^{-}\rightarrow 2NO\uparrow+Fe_2O_3+H_2O \qquad (24)$$

Calcium nitrite competes with the chloride ions for ferrous ions produced in concrete and incorporates them into a passive layer on the iron surface, thus preventing further corrosion. It has been reported that when ZnO was added, the steel remained in passive state reducing Cl^{-} content at reinforcement level, which allows $Ca(NO_2)_2$ to act efficiently on the reinforcement, passivating it.

5.2.1.2 Other inhibitors:

Cementitious-inhibitor systems were effective in inhibiting corrosion compared with the cement coating without an admixture-type inhibitor /**62**/.

The corrosion rate was smaller and the corrosion potential was more positive for the inhibitor-coated sample than the cement-coated samples at equivalent NaCl concentrations. Collins *et al.* **/63/** evaluated several inhibitors such as (1) a calcium-nitrite-based inhibitor, (2) a monofluorophosphate-based inhibitor, (3) sodium tetraborate ($Na_2B_7O_7{\cdot}10H_2O$), (4) zinc borate ($2ZnO{\cdot}3B_2O_3{\cdot}3.5H_2O$), (5) a proprietary oxygenated hydrocarbon produced from an aliphatic hydrocarbon, (6) a proprietary blend of surfactants and amine salts (MCI 2020 which migrate through concrete), and (7) a proprietary alkanolamine inhibitor (MCI 2000). The results of the study, which involved monitoring of corrosion, compressive strength and resistivity, showed that the calcium-nitrite-based inhibitor was the most promising to mitigate corrosion in a repaired structure after removal of chloride-contaminated old concrete. On the other hand, both borate compounds were found to retard the setting of Portland cement.

5.2.1.3 Organic inhibitors:

Electrochemical investigation of water based inorganic material(R2) to inhibit corrosion of steel in concrete showed better performance than alkanolamine inhibitor (M2) on steel specimens immersed in an inhibitor containing 5% NaCl + saturated $Ca(OH)_2$ solutions. Surface analysis indicated that R2 most probably modified the passive film on the steel surface as well as reacted with chloride ions in the vicinity of the metal and stopped them from reaching the surface, whereas M2, which has nitrogen group in its composition, might have modified the passive film on the steel surface and at the same time formed a film on the surface to protect the steel against corrosion in the presence of chloride ions **/64/**. Organic oxygen and chlorine in the composition of M2 could be one of the causes of its inferior performance compared to that of R2. Chromate and water based surface treatment is designed to improve cathodic disbondment resistance and adhesion retention of fusion-bonded-epoxy coatings. Various other factors affect the cathodic-disbondment resistance of epoxy coating rebars. The application temperature and thickness of the coating and steel surface preparation, pH and contamination have a dramatic impact on cathodic-disbondment **/65/**.

5.2.2 Coatings to steel:

A protective anticorrosive treatment to steel reinforcement includes galvanizing, epoxy coating, and cement based coatings. The corrosion protection efficiency of the coating system depends on a number of factors, such as choice of polymer, composition of the coating, method of application and the environment in which it is going to be used. There are a number of metallic coating systems like zinc, nickel, copper, lead and tin. Metals like zinc that are more active than iron will give sacrificial protection. It has been reported that powder epoxies have better overall properties as barrier coatings for reinforcing bars than the tested liquid epoxies. Many coating techniques such as chemical vapor deposition (CVD), physical vapor deposition (PVD), powder slurry, pack cementation, sputtering and molten salts are used to coat steel. However, CVD is too expensive for low cost industrial applications and requires relatively high deposition temperatures. Pack cementation requires high temperatures and long times for coating. Therefore, a detailed study was needed for the development of a suitable coating system for the protection of reinforcing bars.

5.2.2.1 Galvanized coating:

Hot dip galvanizing is a viable means of protecting reinforcement, particularly where the durability of concrete cannot be guaranteed. Its use is considered for aggressive exposure condition. It ensures design strength of concrete and removal of surface rust staining and spalling of concrete.

Properties:

1. Abrasion resistance:- Galvanizing provides a tough, metallurgical bonded zinc coating which completely encloses the steel and consists of a series of inter metallic alloy layers namely eta, zeta, delta, gamma having varying composition of zinc and iron. Microstructures of these layers have hardness more than the base steel thus ensuring a very good abrasion resistance by preventing the peeling of coating. It provides sacrificial protection wherein zinc corrodes preferentially forming a protective cover over areas which are exposed accidentally. Thus, there is no possibility of beneath the layer corrosion.
2. Cathodic Protection: Zinc coating which covers up any scratches that may occur in the coating. This is due to the electrochemical property of zinc which is more electro positive than steel and has a tendency to donate electrons to exposed steel.
3. Uniform coating thickness: The coating thickness remains the same

across the entire length of the bar.

4. Possibility of bending of galvanized steel: the rebars coated can be bent after galvanization without cracking/peeling up of coating because of good ductility.
5. Weldability and bond strength.

5.2.2.2 IPN coating:

A prepolymer of epoxy resin (based on diglycidyl ether of bisphenol A) and phenolic resin (based on cashew nut shell liquid) are made to polymerize with their respective hardeners in such a manner that the prepolymers cross-links simultaneously with their respective hardeners by a separate noninterfering mechanism. The Interpenetrating Polymer Network (IPN) system thus developed has been evaluated for its physicomechanical properties and chemical resistance (against saturated urea solution, diammonium phosphate, 30% sulphuric acid, 30% phosphoric acid, 30% sodium hydroxide solution, and distilled water) as per the relevant standards and has been compared with epoxy coating under a similar set of conditions are reported in Table 9 /**66**/. The basic coating system was modified to make it suitable for the protection of reinforcing steel in concrete. Permeability of IPN is reduced, thus implying reduction in ingress of detrimental ions and ductility is also better than the epoxy system. Hence, the retention of adhesion even at higher fatigue stresses is better. The adhesion test was carried out by bend test as described in IS 13620-1993 /**67**/. Bond strength of the IPN system, both in shear as well as perpendicular to surface, is better than that of epoxy. The chemical resistance of IPN coatings against acids, alkalies, and fertilizers is better than epoxy alone. The above mentioned properties combined with excellent chemical resistance make the IPN system ideal for the protection of steel reinforcement in concrete.

5.2.2.3 Fibre reinforced polymer (FRP) lamination:

Numerous studies have shown that concrete repair using FRP laminates are very successful in restoring or increasing the strength of concrete members. By strengthening concrete members with FRP laminates, concrete spalling and cracking caused by the expansive forces of the corrosion products may be delayed or even prevented. Reinforced concrete beams strengthened with carbon fibre reinforced polymer laminates maintain a high percentage of their undamaged strength, even when subjected to severe rebar corrosion (up to 10% mass loss). The strengthened corroded specimen in this study retained 92% of the control beam strength, while the unstrengthened corroded specimen retained only 79% of the control beam strength. load-deflection curves are shown in Fig. 13 /**68/**.

Table 9

Physicomechanical properties of the coating **/66/**.

Test	**Epoxy System**	**Epoxy/ Phenolic (IPN)**	**Standard**
Tensile Strength (N/mm^2)	22.4	24.4	ASTM D-2370-7
Elongation (%)	8.0	21.0	ASTM D-2370-7
Modulus of elasticity (N/mm^2)	1244.4	1031.0	ASTM D-2370-7
Specific permeability ($mg/cm^2/mm/24$ hr)	0.2043	0.1354	ASTM D-1653-74
Glass transition temperature (°C)	107.0	94.0	DSC method
Coefficient of linear expansion, °C X 10^{-5} (30-80) °C	1.714	0.885	ASTM D-696-7
Shear strength (Kg/cm^2)	58	77	ASTM D-1002-64
Bond strength (Kg/cm^2), steel substrate	25	30	BS 3900-E-10-79
Impact resistance (falling weight method)	No failure	No failure	BS 3900-E-7-74
Scrub resistance (10,000 cycle)	No failure	No failure	ASTM D-2468-79
Salt fog (720 h)	No failure	No failure	ASTM B-117-73
Scratch hardness (1500 g load)	No failure	No failure	BS 3900-E-2-70

5.2.2.4 Titanium dioxide:

Titanium dioxide generally affects the durability of coatings in two distinct and opposing ways: i.e. as a strong UV-absorber, it protects the paint film and as an UV-activated oxidation catalyst, it degrades binders **/69/**. The protective effectiveness of an acrylic dispersion with TiO_2 pigment was the greatest one, resulting in a reduction of 50% in corrosion rate of steel bars corrosion rate and in depth of carbonation, compared to those of the uncoated specimens.

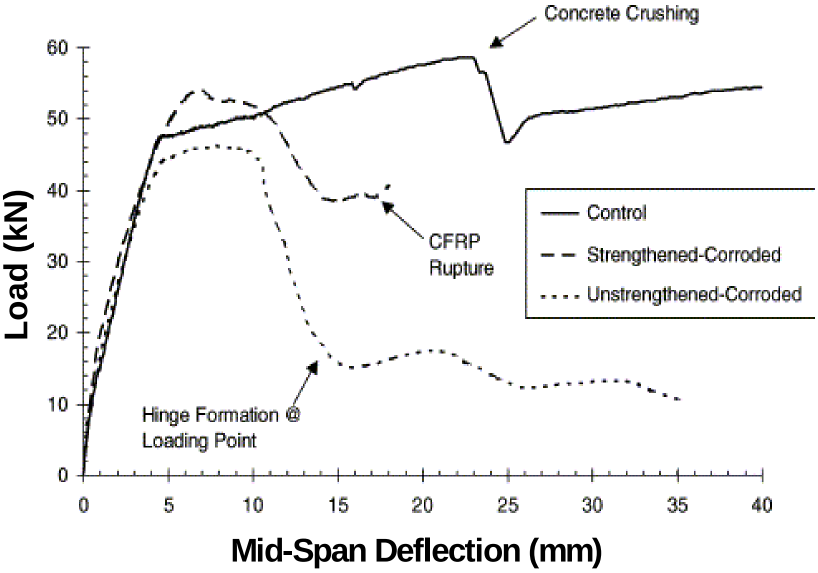

Fig. 13: Load-deflection behaviour for control, strengthened and unstrengthened specimens **/68/**.

5.2.2.5 Cement based coatings:

Since the steel reinforcement embedded in concrete is surrounded by an alkaline medium, a coating based on cement is expected to be more compatible. Cement based coatings **/70/** appear to have better tolerance towards coating damage and, in the presence of damage to the coating, they exhibit better performance in chloride contaminated concrete when compared to epoxy based coatings. Nitrite based inhibitor was dissolved in water and mixed with cement to form a slurry and applied as a coating either by brushing or dipping. Inhibited cement slurry coating is an inorganic coating system and is applied in four steps viz. pickling, phosphating, application of two coats of inhibited cement slurry coating and sealing **/71/**. Since this coating is applied at site, damage due to transport and lifting are greatly minimised. It has a minimum durability factor of 25 **/72/**. The durability factor is defined as the corrosion rate of uncoated rebar to the corrosion rate of coated rebar under similar test condition. The inhibited cement slurry coating protects the steel by creating a passive environment with a high tolerance towards chloride. Sealing of the pores in the coating is effected by giving a silicate based treatment. This treatment seals as well as hardens the coating.

5.2.2.6 Silicon and silicon-titanium protective coatings:

This coating increases the corrosion resistance at temperatures around 550 °C. The steel samples were immersed in a bed of silicon or silicon-titanium particles fluidized by an argon –0.1% HCl mixture and kept at temperatures ranging from 400 to 750 °C **/73/**. Coatings rates of over 1 μm min^{-1} were obtained at the highest temperatures.

5.2.2.7 HP/HVOF:

The stainless steel coating prepared using the high pressure/high velocity oxygen fuel (HP/HVOF) process has superior polarization resistance compared to that prepared using the twin wire electric arc (TWEA) process **/74/.** HP/HVOF produces a dense, low-oxide-content coating while TWEA produces relatively more porous coatings, thus making the former a better option.

5.2.2.8 Acrylic latex coatings (ALC):

It greatly reduces the corrosion rate of steel rebars. ALC is a copolymer of methyl methacrylate, butyl methacrylate and acrylic acid (50:50:1). The solid content is 42%. It is neutralized to weak alkalinity by triethnolamine before use. Two methods are employed to improve corrosion resistance namely by adding corrosion inhibitive pigments, such as zinc yellow or red, the latex is led to passivate the steel surface, or by modifying the latex with silane or mercapto compound to reinforce the steel/coating interface **/75/**.

5.2.2.9 Epoxy coating:

Fusion bonded epoxy coating is a process where epoxy powder is applied by electrostatic spray on hot steel at a pre-set temperature. The powder, when in contact with the hot bar, melts, flows, gels and cures to a well-adhered continuous corrosion resistant protective coating. Epoxy coated bars, with a coating thickness of 200 – 300 μm remained practically unaffected under natural and accelerated exposure conditions and maintained all the original characteristics of gloss, coating hardness and coating adhesion even with as small a cover as 20 mm **/76/.**

5.3 Cathodic protection:

Due to the physical, chemical and electrical properties of the concrete, impressed current cathodic protection is the only effective means of controlling corrosion within chloride contaminated concrete. The cathodic protection is the reduction of the corrosion rate by making the electrode potential of the rebar more negative so that the current at any anode is reduced while that at any cathode is increased. In the case of reinforced steel structures, problems arise due to resistance fluctuations as dry concrete has high resistance and wet concrete has low resistance. If the applied voltage is kept constant, more cathodic protection current flows under dry conditions. Because of these resistance changes, design of cathodic protection for reinforced steel in concrete structures is considerably more difficult than for soils or sea water.

6.0 CONCRETE FOR NUCLEAR REACTORS

6.1 Aging of Nuclear Power Plant Concrete Structures:

One of the primary factors that could affect the continued operation and development of nuclear power relates to aging of the plants and its potential impact on performance. Nuclear power plants are designed, built and operated to standards that aim to reduce the releases of radioactive materials to levels as low as reasonably achievable. Nuclear power plants, however, involve complex engineering structures and components operating in demanding environments that potentially can challenge the high level of safety required throughout the operating life of a plant. Therefore, it is necessary that safety issues related to plant aging and extended service of nuclear plants be resolved through development of sound scientific and engineering understanding. Nuclear safety-related concrete structures are composed of several constituents that perform multiple functions such as foundation, biological shielding, containment, protection against internal and external hazards load-carrying capacity, radiation shielding and leaktightness.

The constituents for constructions of nuclear reactors include concrete, conventional steel reinforcement, prestressing steel, and steel liner materials. The concretes typically consist of a moderate heat of hydration cement, fine-aggregates (sand), water, various admixtures for improving properties or performance of the concrete. Degradation is considered to be any phenomenon that decreases the load-carrying capacity of a containment, limits its ability to contain a fluid medium or reduces the service life. The root cause for containment degradation can generally be linked to a design or construction problem, inappropriate material application, a base-metal flaw, insufficient maintenance or inspection activities or excessively severe service conditions. Primary mechanisms or factors that can produce premature deterioration of concrete structures include those that impact either the concrete or reinforcing steel materials. Degradation of concrete can be caused by adverse performance of either its cement-paste matrix or aggregate materials under chemical or physical attack. Chemical attack may occur in several forms like leaching, sulphate attack, attack by acids and bases, salt crystallization and alkali-aggregate reactions. Physical attack mechanisms for concrete include freeze/thaw cycling, thermal exposure/ thermal cycling, abrasion/erosion/cavitation, irradiation and fatigue or vibration. Degradation of mild steel reinforcing materials can occur as a result of corrosion, irradiation, elevated temperature or fatigue effects. Prestressing materials are susceptible to the same degradation mechanisms as mild steel reinforcement, plus loss of prestressing force, primarily due to tendon relaxation and concrete creep and shrinkage. Steel containment degradation can be classified as either material or physical damage. Material damage occurs when the microstructure of the metal is modified causing changes in its mechanical properties. Degradation mechanisms that can potentially cause material damage to containment steels include: low-temperature exposure, high-temperature exposure, intergranular corrosion, dealloying corrosion, hydrogen embrittlement and neutron irradiation /77/. Physical damage occurs when the geometry of a component is altered by the formation of cracks, fissures or voids or its dimensions change due to overload, buckling, corrosion, erosion or formation of other types of surface flaws. Changes in component geometry, such as wall thinning or pitting caused by corrosion, can affect structural capacity by reducing the net section available to resist applied loads. In addition, pits that completely penetrate the component can compromise the leak-tight integrity of the component. Primary degradation mechanisms that potentially can cause physical damage to containment pressure boundary components include: general corrosion, (atmospheric, aqueous, galvanic, stray-electrical current and general biological) localized corrosion, (filiform, crevice, pitting and localized biological) mechanically assisted degradation (erosion, fretting cavitation, corrosion fatigue, surface flaws, arc strikes and overload conditions); environmentally induced cracking (stress-corrosion and hydrogen-induced); and fatigue. Material degradation due to either general or pitting corrosion represents the greatest potential threat to the containment pressure boundary. From a safety point of view, the containment is one of the most important components of a nuclear power plant because it serves as the final barrier to the release of fission products to the outside environment under postulated accidental conditions. Ensuring that the structural capacity and leak-tight integrity of the containment has not deteriorated to unacceptable levels due either to aging or environmental stressor effects is essential to reliable continued service evaluations and informed aging management decisions. Concrete surrounding the pressure vessel of a nuclear reactor as a shielding material is exposed to nuclear radiation such as neutrons and gamma rays. Irradiation of fast neutrons to a dose of more than ~10^{19} n/cm^2 causes the deterioration of concrete **/78/.** Irradiation results in the expansion of aggregates and the shrinkage of cement paste. The expansion at a dose of 5 x 10^{19} n/cm^2 is about 1% for limestone and flint, and is 0.1% for serpentine. The degradation of the mechanical properties of concrete by fast neutron irradiation is higher for concrete showing higher degree of expansion due to the acceleration of alkali-silica reaction of aggregates.

6.2 Inspection of Nuclear Power Plant containment structures:

Primary objectives for testing concrete structures include determination of strength, comparative quality assessments, examination of local integrity, assess potential durability and identify causes of deterioration. The distress that can occur in concrete materials includes cracking, chemical deterioration, delaminations and strength losses. Methods used to detect discontinuities in concrete structures are either direct or indirect. The direct method involves a visual inspection of the structure, removal/testing/analysis of materials. The indirect methods measure some parameter from which an estimate of the extent of degradation can be made through existing correlation.

Table 10

Recommended testing methods to access concrete degradation.

S. No	Degradation Factor	Symptom	Testing Methods	
			To identify occurrence	**To access extent of damage**
1.	AAR	Cracking expansion	Core petrography	1.Visual and petrography 2. pulse velocity 3. impact echo 4. pulse echo 5. modal analysis
2.	Sulphate attack	Cracking expansion	1. Core petrography 2. Core chemical	1.Visual and petrography 2. pulse velocity 3. impact echo 4. pulse echo 5. modal analysis
3.	Efflorescence and leaching	Sulphate deposits of efflorescence	1.visual 2.core petrography 3.sample x-ray diffraction	1.Visual and petrography
4.	Bases/acids/salt crystallization	Disintegration and loss of paste	1. core petrography 2. chemical analysis	1.Visual and petrography
5.	Freeze thaw	Scaling, Spalling, Cracking	1.visual 2.core petrography	1.Visual and petrography 2. pulse velocity 3. impact echo 4. pulse echo

Table 10 (continued):

6.	Thermal irradiation	Spalling, Cracking, Loss of strength	1.visual 2.core petrography	1.Visual and petrography 2. pulse velocity 3. impact echo 4. pulse echo
7.	Fatigue vibration	Micro Cracking, Cracking, Excessive deflection	1.visual 2.core petrography	1.Visual and petrography 2. pulse velocity 3. impact echo 4. pulse echo 5. modal analysis
8.	Creep	Cracking, Excessive deflection	1. visual	1.Visual and petrography 2. modal analysis
9.	Reinforcement corrosion	Corrosion	1.visual 2.core petrography 3. electrical methods 4. chemical methods 5. air permeability 6. nuclear (moisture content)	1. visual and petrography 2. impact echo 3. pulse echo 4. radiography
10		Cracking Delamination	1. visual 2. core petrography 3. impact echo 4. pulse echo 5. Audio methods	1. visual and petrography 2. impact echo 3. pulse echo 4. pulse velocity 5. audio methods 6. infrared thermography

Nondestructive test methods can be used to indicate the strength, density and quality of concrete, locate voids or cracks in concrete and locate steel reinforcement and indicate depth of concrete cover. Visual inspection, audio, infrared thermography, magnetic methods, stress wave transmission, ground-penetrating radar, tomography, rebound hammer, ultrasonic pulse velocity and modal analysis are some of the techniques used for inspection of concrete. Electrochemical technique such as potential measurements and radiography are used to constantly monitor the health of the mild steel reinforcement.

Destructive test methods can be utilized to determine concrete strength, density and quality; locate voids or cracks in concrete; locate steel reinforcement and determine depth of concrete cover and detect corrosion of steel reinforcing materials. Destructive testing techniques include air permeability, break-off, core testing, probe penetration, pullout, chloride-ion content, carbonation depth and petrography. Table.10 shows the testing methods to assess concrete degradation **/79/.**

7.0 PROBABILISTIC LIFETIME DESIGN OF CONCRETE STRUCTURES

The aim of this part of the review is to explain the influence of the exposure conditions for reinforced concrete structures and the consequences on their expected service life. The life-time of a concrete structure can be modelled as series of limit-states. Four major limit-states can be identified in the life-time of a concrete structure:

a) **Initiation of corrosion –** Initiation either by carbonation or chloride ingress. This limit state gives the time when the carbonation front reaches the reinforcement or the chloride threshold level is exceeded at the reinforcement.

b) **Cracking –** Cracks appear because corrosion has been going on for a while, and are caused when corrosion products have expanded to the extent that cracks start to develop in the concrete. This limit state gives the time when the first crack due to corrosion appears.

c) **Spalling –** Spalling occurs when the cracks have grown to a certain level and the concrete cover starts to spall. This limit state gives the time when spalling due to corrosion first occurs.

d) **Collapse –** Collapse occurs when the reinforcing bars start to yield, due to loss of cross-section area caused by corrosion, and lose their load-carrying ability. This limit state gives the time when the reinforcing bars start to yield.

7.1 Environmental influence on the life-time models

The environment influences the life-time models in three ways:

a) **Driving potential in diffusion –** Influence of the potential in the diffusion of carbon-dioxide and chloride into the concrete.
b) **Diffusion coefficient –** The transport properties of the concrete are mainly influenced from the moisture and temperature conditions in the concrete.
c) **Corrosion properties of the concrete –** The corrosion of the rebars is influenced by the moisture and temperature conditions in the concrete.

8.0 SERVICE LIFE PREDICTION OF A CORRODING RC STRUCTURE

There are several ways of predicting service life due to the corrosion damage of reinforcement in concrete using different deterioration models. For a corroding structure, the residual service life at any time may be taken as the time remaining for the crack to develop at concrete surface due to the rust expansion. There are various models available in the literature for service life prediction. Besides these models, experimental techniques are also available for predicting service life. Some of the models and an experimental technique for service life prediction are summarized.

8.1 Tuuti's Model

Tuuti **/80/** suggested a model for predicting the service lives of reinforced concrete structures in Fig. 14. The deterioration of reinforced concrete structures is a time dependent process, which takes place as a number of chemical, electro-chemical and physical processes. The maximum acceptable corrosion level is related to the appearance of cracks. The deterioration process consists of two periods: initiation and propagation. The length of the initiation period is estimated from the time required for aggressive species to reach reinforcement surfaces and trigger active corrosion, while that of the propagation period is the time elapsed after initiation till repair becomes mandatory.

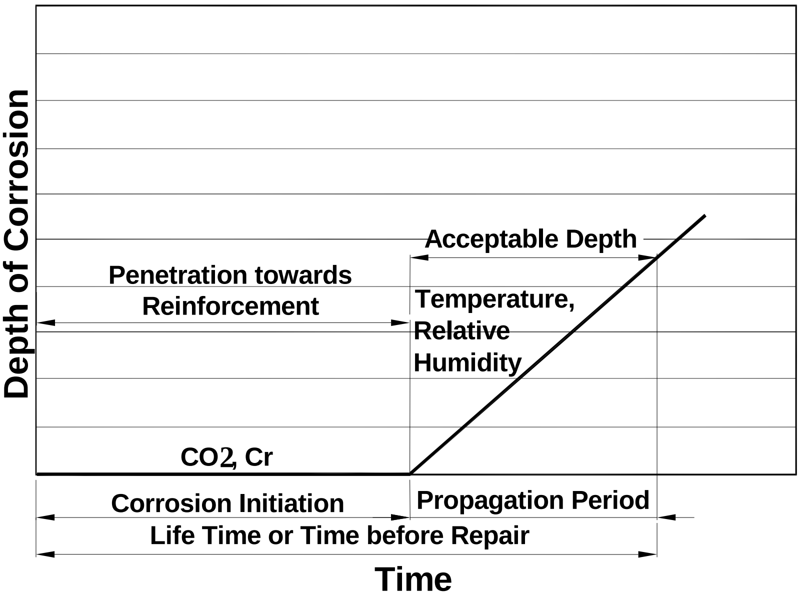

Fig. 14: A schematic sketch of steel corrosion sequence in concrete.

8.2 Cady and Weyers Model

Cady and Weyers /**81**/ developed a deterioration model to estimate the remaining life of concrete bridges in corrosive environments. The model has three phases: diffusion, corrosion and deterioration as shown in Fig. 15. Diffusion describes the time for chloride ions to penetrate the concrete cover and to initiate corrosion. The diffusion time usually can be determined empirically using Fick's Second Law. Corrosion defines the time period between initiation of corrosion to first cracking of concrete cover. The time to cracking ranges from 2 to 5 years. Deterioration describes the time for damage to reach a level which is deemed as the right time for repair or rehabilitation. According, to Cady-Weyer's model, the corrosion rate is the key to predicting the time to cracking. The corrosion rate is largely controlled by the rate of oxygen diffusion to the cathode, resistivity of the pore solution and temperature.

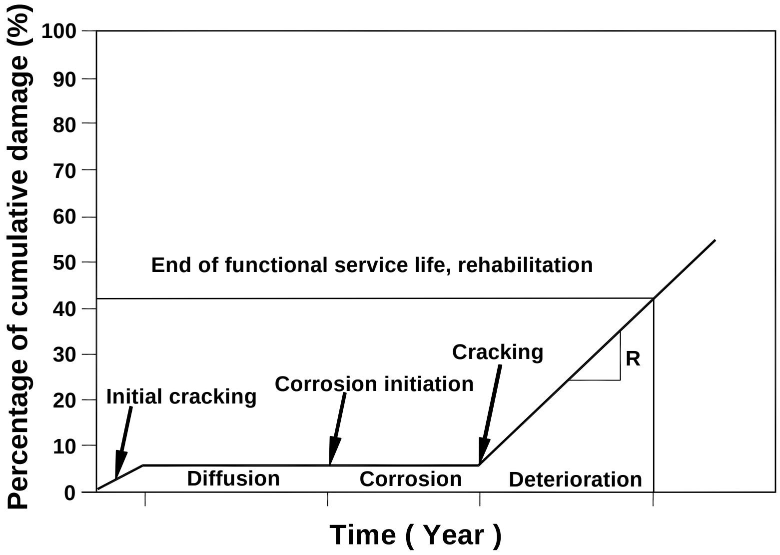

Fig. 15: Chloride corrosion deterioration process for a concrete element with a mean cover depth of 2 in.

8.3 Bazant's Mathematical Model

Bazant's model **/82/** for the prediction of corrosion damage considers the volume expansion due to the formation of hydrated red rust, ($Fe(OH)_3$), over the residual rebar core. This red rust is expansive in nature and occupies four times the volume of parent steel. Thus, a uniform radial pressure is exerted onto the surrounding concrete resulting in outward radial deformation of concrete. This deformation is same as the increase in diameter ΔD of the rebar (due to deformation compatibility) and increases with an increase in the volume of rust till the cover concrete cracks and is rendered functionally unsatisfactory.

The time of corrosion to cracking, t_{cr}

$$t_{cr} = \rho_{cor} D \, \Delta D / S \, j_r \qquad (25)$$

where S is the bar spacing, D is the diameter of the bar, ΔD is the change in diameter of the bar, j_r is corrosion rate of steel, and ρ_{cor} is a function of the mass densities of steel and rust.

$$j_r = (W / F)\, I_{corr} \tag{26}$$

where $j_r =$ instantaneous corrosion rate (gm/cm^2/s), W = equivalent weight of steel, F = Faraday's constant = 96487 C, I_{corr} = corrosion current density (Amp/cm^2)

According to Bazant's models, the time to cracking is a function of corrosion rate, spacing of rebars and certain mechanical properties of concrete such as tensile strength, modulus of elasticity, Poisson's ratio and creep coefficient. The predicted time to cracking calculated from Bazant's model is much shorter than the observed one.

8.4 Morinaga's Empirical Equations

Morinaga **/83/** developed an empirical equation to compute the amount of corrosion, Q_{cr}, when concrete cover cracks due to expansion by means of rust formation on rebar surface.

The expression to estimate, Q_{cr}, is:

$$Q_{cr} = 0.602d\, (1 + 2c /d)^{0.85} \tag{27}$$

where

Q_{cr} is the critical mass of corrosion products (10^{-4} g/cm^2)
c is the cover to the reinforcement (mm)
d is the diameter of reinforcing bars (mm)

The time for cracking to take place is given by:

$$t_{cr} = Q_{cr} / i_{cor} \tag{28}$$

where i_{cor} is the corrosion rate in gram per day, t_{cr} is the time to cracking in days. According to Morinaga's equations, the time to cracking is a function of the corrosion rate, concrete cover depth and reinforcing size.

The predicted time to cracking calculated from Bazant's and Morinaga's model is much shorter than the observed one due to the complexity of compositions and properties of corrosion products, corrosion processes and both empirical equations are based on the steady state corrosion process to calculate the time to cracking.

8.5 Wang and Zhao's model

Wang and Zhao **/84/** have suggested a step method of using finite element analysis to determine the thickness of the corrosion product, Δ, corresponding to the time duration when the surface concrete cracks. They have established an empirical expression to determine the ratio of thickness of corrosion product, Δ, to the depth of rebar penetration, H, corresponding to the cracks in cover concrete. The ratio (Δ/H), as given below, is termed as expansion coefficient, γ and has been expressed as a function of cube strength of concrete, f_{cu}, as:

$$\Delta/H = \gamma = 0.33\,(D/C_v)^{0.565}\,f_{cu}^{1.436} \qquad (29)$$

Using the value of Δ obtained through the finite element model, the value of H corresponding to cracks in cover concrete can be obtained. Further, the value of H can be used to determine the time necessary for longitudinal cracking of concrete cover, t_{cor} as:

$$t_{cor} = H / P_r \qquad (30)$$

where P_r is penetration rate of rebar due to corrosion.

$$P_r = (\,W / F\rho_{st}\,)\,I_{corr} \qquad (31)$$

where W = equivalent weight of steel, F = Faraday's constant = 96487 C, ρ_{st} = density of steel, I_{corr} = corrosion current density (Amp/cm^2)

The model suggested by Wang and Zhao can be used only in conjunction with the finite element model requiring the determination of Δ.

8.6 Dagher and Kulendran's model

Dagher and Kulendran **/85/** have also carried out a finite element modeling of corrosion damage in concrete structures. This numerical model is rather versatile in terms of estimating the radial bar expansion Δ, and includes: (a) a number of options for modeling crack formation and propagation, (b) the capacity to accept any shape of corrosion around the rebars, (c) the ability to incorporate dead and live load stress and initial shrinkage and temperature related cracks in the analysis, and (d) pre and post processing modules which offer automatic mesh generation and visual representation of crack propagation.

In the context of service life prediction of RC structures subjected to rebar corrosion, this model can be used more reliably to determine the radial bar expansion Δ, at which the cracks in cover concrete would occur. However, their work will require extension to make it capable of service life prediction.

8.7 Ahmad's Model

Ahmad *et al* suggested an experimental method for service life prediction based on cumulative damage theory **/86/.** The model aims to calculate the total life of steel against corrosion cracking of cover concrete, L_t.

A reinforced concrete specimen is allowed to corrode for a time duration, L_c, at its natural corrosion rate, I_{corr}, from the time of depassivation, tp, onward and then the same is subjected to an impressed anodic current, I_a, up to the time of cracking, t_{cor}, of cover concrete.

According to the cumulative damage theory,

$$(L_c / L_t) + (L_a / L_l) = 1 \tag{32}$$

where L_c/L_t is fraction of damage due to the natural corrosion, L_a/L_l is fraction of damage due to externally applied current. L_a is the time taken by the specimen for its complete damage under the effect of external current and the natural corrosion that had already taken place. L_l is the time taken by the specimen for its complete damage under applied current alone excluding the effect of natural corrosion.

The total life of specimen against corrosion cracking of cover concrete, L_t is:

$$L_t = L_c / [\, 1 - (K_2/K_1)\{F_0 f(C_v/D) / EI_a\}] \tag{33}$$

where $f(C_v/D)$ is a function of the ratio of cover thickness, C_v, to the rebar diameter, D. E is modulus of elasticity of concrete, K_1 and K_2 are constant.

8.8 Marios Chryssanthopoulos and Garry Sterritt Model

The deterioration of reinforced concrete structures due to chloride ingress can be divided into two phases, initiation and propagation. This entails modeling the corrosion initiation stage using Fick’s second law of diffusion and the propagation stage through a corrosion penetration/loss relationship. Marios Chryssanthopoulos and Garry Sterritt derived an alternative solution to Fick’s second law by considering the transport mechanisms involving diffusion as well as absorption and deterioration processes as concrete cover and exposure conditions **/87/.**

$$C(x,t) = M/(\pi Dt)^{1/2} \exp(-x^2/4Dt) \qquad (34)$$

C(x,t) = chloride concentration at depth x after time t. M = quantity of accumulated chloride on concrete surface per unit time in $kg/m^2/yr$

Critical chloride corrosion threshold (C_{th}) varies with temperature, W/C ratio, humidity, oxygen, water content, pH and % of free chlorides, where free chlorides are taken as one third of the total chlorides present. A semi-empirical equation is developed to estimate the time to delamination after corrosion initiation,

$$T_{DEL} = \{ V_{DEL} / C_R * 1.25\ D\} \qquad (35)$$

T_{DEL} = delamination time (yrs)
V_{DEL} = delamination volume per unit length of bar (mm^3/mm)
C_R = corrosion rate (mm/yr)
D = rebar diameter (mm)

and 1.25 factor is related to the position of the assumed fracture plane of the bar.

8.9 Andrade and Clear Model

Andrade and Clear /**88**/ suggested a model to estimate the remaining service life of reinforced concrete in which corrosion is the limiting degradation process. This is one model used the polarization resistance technique to measure corrosion currents. Andrade's model considers reduction of the steel section as the significant consequence of corrosion instead of cracking or spalling of concrete

$$D(t) = d(0) - 0.023 * I_{corr} * t \qquad (36)$$

where
d(t) = the reinforcement diameter in mm at time (t) in years after the beginning of propagation period.
d(0) = the initial diameter of the reinforcement in (mm)
I_{corr} = the corrosion rate in (A/cm^2)
0.023 = the conversion factor of A/cm^2 into mm/year.

Both the models assume the linear change of corrosion rate with time. Due to the influence of the environmental conditions the linearity of the change of corrosion rate with time cannot be expected.

8.10 Poulsen Model

Poulsen developed a model which takes the above-mentioned problem into account.

$$D = 2 * 10^{-3} * K * R(t) * t \qquad (37)$$

where
D is loss of diameter (mm) with time
K is correction factor,
R(t) is corrosion rate at time t (μm/year)

The calculation by this model showed promising results.

8.11 Koji Takewaka et al /89/

These workers constructed a simulation model that includes a penetration model of corrosion factors and a corrosion model of reinforcement as shown in Fig. 16.

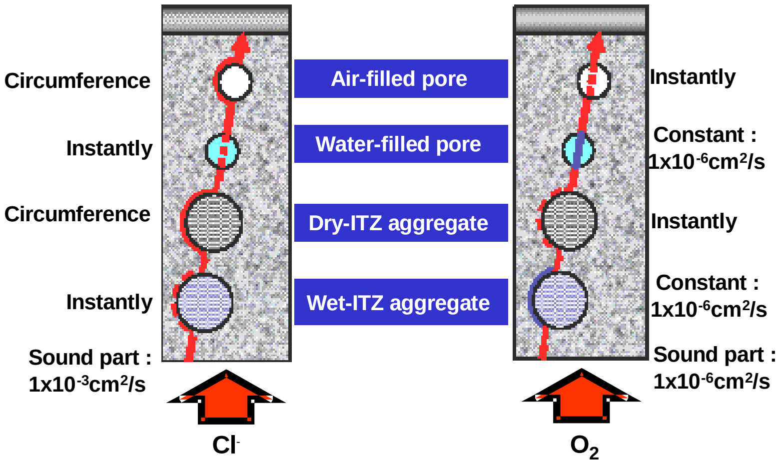

Fig. 16: Diffusion path of Cl^- and O_2.

Chloride penetration model:

The penetration of chloride ions is one of the most influential factors for the corrosion of reinforcing bars. It is assumed that chloride ions penetrate concrete through a straight path according to Fick's diffusion theory using diffusion coefficient for the sound parts of concrete.

$$T = L^2 / 12\, D_{CL}[1 - (C_L/C_0)^{1/2}] \tag{38}$$

where

T is diffusion time to chloride ion to rebar (sec)

D_{CL} is Cl^- diffusion coefficient in sound concrete (m^2/s)

L is length of chloride diffusion route assumed in the model (m)

C_0 is chloride concentration of concrete surface

C_L is chloride concentration at threshold value of steel.

Penetration model of oxygen:

The penetration of oxygen also affects the progress of corrosion of reinforcement in concrete. Oxygen is assumed to penetrate into concrete through a straight route. The effective diffusion coefficient of oxygen is obtained by this equation,

$$D_{OA} = D_{OC} * (L_R / L_X)^2 \tag{39}$$

where

D_{OC} = diffusion coefficient of oxygen in sound concrete (m^2/s)
L_R = thickness of cover concrete (m)
L_X = length of oxygen diffusion path assumed in the model (m)

Using the reaction rate, the amount of corrosion loss generated per unit time and sum amount of corrosion are obtained by the following equation,

$$C_T = V^{Fe2+} .[Fe] \tag{40}$$

$$C_V = \Sigma C_T \,.\, \Delta T \tag{41}$$

where
V^{Fe2+} is the reaction rate of Fe $^{2+}$
C_T is the amount of corrosion in unit time
C_V is sum amount of corrosion.

Besides chloride and oxygen, water also has a large influence on the reinforcement corrosion reaction.

$$C'_V = C_V * W_s / W_N \tag{42}$$

C'_V = corrected sum amount of corrosion
W_s =amount of water in diffusion layer around each reinforcement section (m^3)
W_N = amount of sufficient water for C_v

This simulation method can be made more effective for evaluating the durability of concrete structures.

8.12. Youping Liu Model

Youping Liu suggested an experimental model to predict the time-to-corrosion cracking of the cover concrete in chloride contaminated reinforced concrete structures. The proposed model is based on the fact that corrosion rate is a function of the temperature, ohmic resistance of concrete, chloride content and corrosion time related to the service conditions of concrete structure. Based on annual mean temperature, ohmic resistance of concrete and chloride content for the reinforced concrete, the corrosion rate can be predicted by the model /**90**/.

$$i_{corr} = k\, e^{-Q/RT}\, (cl^{-})^{m}\, (t)^{n}\, (R_c)^{l} \tag{43}$$

where
i_{corr} is the corrosion rate (mA/sq.ft)
Cl^- is chloride content (lb/yd^3)
T is temperature at the depth of steel surface (in deg K)
R_c is ohmic resistance of concrete (Ohms)
t is corrosion time (year)

Model Interpretations:

*Temperature***:** In general, corrosion rate rises as the temperature increases but, the overall effect of temperature on corrosion rate in concrete is very complex and controlled by interactions among other factors.

*Ohmic resistance of concrete***:** Corrosion rate of steel in concrete increases as concrete ohmic resistance decreases.

Chloride content: The value of corrosion rate increases as the amount of chloride content increases in concrete. This is due to the increase of conductivity of concrete as chloride ions increase.

*Exposure time***:** Corrosion exposure time has significant effect on the corrosion rate during early stages after corrosion initiation. The corrosion rate decreases rapidly at the early stage and then tends to reach a near constant value due to the changes of ratio of anode and cathode areas and from the formation of the rust products on the steel surface.

The calculated corrosion rates by this model are developed from the admixed chloride concrete and found about 1.5 to 1.6 times higher than that from weight loss. Further work needs to be done on determining the difference in chloride concentration in concrete pore solution between admixed chloride concrete and field concrete.

The *corrosion-cracking model* proposed by Youping Liu **/90/** shows that the critical mass of the corrosion products (W_{crit}) to induce cracking of the cover concrete has two parts, the amount of corrosion products to fill the total interconnected pores around the steel/concrete interface (W_p) and the amount of corrosion products to generate the critical stress (W_s).

$$W_s = \rho_{rust} [\ \pi(D + 2d_0)d_s + (W_{st} / \rho_{st})] \tag{44}$$

where
ρ_{rust} = the density of corrosion products
ρ_{st} = the density of steel
d_0 = the thickness of pore band around the steel/concrete interface
d_s = the thickness of corrosion products to generate the tensile stresses
D = diameter of steel reinforcement
W_{st} = mass of steel corroded

The critical amount of corrosion products is given by:

$$W_{crit} = \rho_{rust} [\ \pi(d_s + d_0)D + (W_{st} / \rho_{st})] \tag{45}$$

W_{st} , the amount of steel corroded equals αW_{crit} where, α is the molecular weight of steel divided by the molecular weight of corrosion products.

$$W_{crit} = \rho_{rust} [\ \pi\{(Cf_t / E_{ef}) ((\ a^2 + b^2 / b^2 - a^2\ ) + \nu_s) + d_0\}D + (W_{st} / \rho_{st})] \tag{46}$$

The critical amount of corrosion products needed to induce cracking of the cover concrete is mainly dependent on the tensile strength of concrete, cover depth, elastic modulus of concrete and properties of steel/concrete interface.

The rate of rust production is given by:

$$dW_{rust} /dt = K_p / W_{rust} \tag{47}$$

where W_{rust} is amount of rust products, t is corrosion time and K_p is the rate of rust production which is related to the rate of metal loss expressed in terms of corrosion rate,

$$K_p = 2.59 * 10^{-6} (\ 1/\alpha)\pi D\ i_{cor} \tag{48}$$

where, α is related to types of rust products, D is the steel diameter and I_{cor} is the annual mean corrosion rate. By knowing the corrosion rate, the amount of rust products for a certain period of corrosion can be estimated.

When the total amount of corrosion products reaches the critical amount of rust products, the internal expansion stress will exceed the tensile strength of concrete and cause the cracking of the cover concrete.

The time to cracking is given by:

$$T_{cr} = W^2{}_{crit} / 2K_p \tag{49}$$

where W_{crit} is the critical amount of corrosion products.

The time to corrosion cracking model developed here shows that the time to corrosion cracking of the cover concrete in a chloride contaminated concrete structure is a function of corrosion rate and critical mass of the corrosion products. The time to cracking predicted by the model are in good agreement with the observed times to cracking based on this study.

The proposed corrosion-cracking model for predicting time to cracking is limited to the corrosion damage caused by the volume increase from the formation of rust. In the field situation, other factors such as freezing-thawing may act simultaneously with the corrosion which may accelerate the cracking process. Much work is required on the corrosion cracking under the dynamic loading.

Modeling of Alkali-aggregate reaction in concrete structures:

8.13 B. Capra and J.P. Bournazel Model

AAR is modelled by a global kinetics concept which includes chemical reactions, temperature, humidity effects and stress **/91/**.

$$\varepsilon^{aar} = \varepsilon^{aar}(\, A,T,H,\sigma \,) \tag{50}$$

The evolution of the expansion related to the reactivity potential will be:

$$\varepsilon^{arr}(t,T) = \varepsilon_0 / A_0 \,(1 - A_0 - e^{-x}) \qquad \text{if } A > A_0 \tag{51}$$

where $x = k_0.e^{-Ea/RT}.\ T$

and A is rate of reaction, ε^{arr} is the strain due to AAR and ε_0 is the free expansion.

$$\varepsilon^{arr}(t,T) = 0 \qquad \text{if } A < A_0 \tag{52}$$

where ε_0 and A_0 are dependent on concrete material properties such as porosity.

The evolution of the expansion and the relative humidity (RH) can be modeled by a simple power function,

$$\varepsilon^{aar}/\varepsilon_{100} = H^m \qquad (m = 8) \tag{53}$$

where H is the relative humidity andε_{100} the free expansion at H = 100 %

The evolution of the irreversible strains due to AAR is :

$$\varepsilon^{aar}(A,T,\sigma,t) = H^m.\ \varepsilon_0 / A_0\ (1 - A_0 - e^{-x}).\ f(\sigma) \tag{54}$$

where σ is the applied stress.

This model postulates a decrease of expansion due to an applied stress.

8.14 Bruno Capra and Alain Sellier Model

This model makes it possible to perform numerical simulations of a reinforced concrete subjected to both AAR and mechanical loading. The results are achieved in terms of damage index and swelling fields **/92/.**

$$\varepsilon_i = \varepsilon_i^{e} + \varepsilon_i^{pl} + \varepsilon_i^{AAR} \tag{55}$$

The total strains ε_i are supposed to be the sum of the elastic strain ε_i^{e}, the mechanical anelastic strains ε_i^{pl} (without AAR) and of the strains due to AAR ε_i^{AAR}.

This modelling of AAR is based on a global description of the chemical kinetics of the reactions and on a physical description of the swelling mechanisms. The method employed to take into account the coupling between chemical and mechanical phenomena leads to a model, which integrates the various possible sources of concrete damage. The numerical simulations showed a good agreement between experiments and the model responses in term of three-dimensional swelling under different loading levels.

8.15 Ulm Model

Farage, Alves and Fairbairn /**93**/ have reported that Ulm *et al*. developed a one-dimensional model of expansive concrete behaviour. According to this model, concrete is considered as a porous medium comprising a solid matrix skeleton with gel occupying the voids, giving way to the concept of total stress (σ) acting on a unit volume of concrete and gel, effective stress (σ_μ) acting on the solid matrix and pore pressure (p_g) in the gel.

$$p_g = E_g(\varepsilon_{ch} - \varepsilon) \tag{56}$$

where, ε_{ch} is the AAR –induced strain, ε is the concrete skeleton strain and E_g is the gel elastic modulus.

The material total strain ε is the superposition of elastic strain (ε^e) and postcracking strain (ε_{cr}).

$$\varepsilon = \varepsilon^e + \varepsilon_{cr} \tag{57}$$

A macroscopic AAR model was developed within the framework of a smeared crack finite element approach. Comparison between the obtained results and available experimental information shows that the implemented model adequately represents an important feature of AAR-affected concrete—unloading and reloading behaviour.

The adapted smeared crack model derives from the concept of cohesive cracking proposed by Hillerborg *et al*. **/94/** integrated to the crack band model presented by Bazant and Oh **/95/**. The energy release rate G_f is an intrinsic parameter that governs crack opening in concrete. This parameter is the energy required to crack a unit area of the material and is represented by the material's stress–displacement relationship, from which the stress–strain relationship is obtained through a characteristic width h, which is a region of the finite element where crack opening is considered to process.

$$\sigma_\mu = D\varepsilon \tag{58}$$

As soon as cracking is detected, directions normal to the crack surfaces are considered as uncoupled to the other directions, since the model does not take shear stresses in the cracked planes into account. The uncoupling is introduced in the system by replacing the initial elastic matrix D by D_{cr} in which all terms related to direction couplings are null. The model allows a maximum number of three cracks per element and, from crack formation on, calculations are made in the local reference system

$$\sigma_I = D_{cr}\varepsilon_I \qquad I = 1,2,3 \quad (59)$$

Further studies concerning the coupling between stresses and AAR should be developed to extend the model application to structures under more sophisticated loading and boundary conditions.

Modeling carbonation of concrete structures:

8.16 Lindavall's Model -- Temperature effect on CO_2 diffusion

The solubility of CO_2 is decreased and acid formation is also decreased, but diffusivity of CO_2 is increased due to increased activity energy with increase in temperature. The temperature dependence on diffusion follows Arrhenius's Law. It has been shown that activity energy of CO_2 is almost constant in certain temperature range (20 - 40 °C) regardless of W/C ratios of concrete. The temperature effect on diffusivity of CO_2 is given

$$D(T) = D_{ref} \,.\, \exp[U/R\ \{(1/T_{ref}) - (1/T)\}] \quad (60)$$

where D_{ref} is reference diffusivity (same as DCO_2^{eq} in cracked concrete and DCO_2 in sound concrete), U (8500 Cal/mol K) is activity energy of CO_2, and T_{ref} (298 K) is reference temperature.

The proposed model by Anders Lindvall is mathematically represented by

$$x_c\ [(2k_1k_2D_{eff}C_s)^{1/2} / a]\ (t^{1/2})[(t_0)^n / t] \quad (61)$$

where D_{eff} is the effective diffusion coefficient at a defined execution and environmental conditions, a is the binding capacity for CO_2 , t is the time in service, t_0 is a reference period, k_1 is a factor which considers the influence of execution of D_{eff} (influence of curing), k2 is a factor which considers the influence of the environment on D_{eff} (influence from moisture and temperature conditions at the surface of the concrete structure) and n is a factor which considers the influence from the environment on the time-evolution of D_{eff} **/96/**.

8.17 Saetta Model

Bazant **/82/** defined a one-dimensional case to predict the carbonation process, which overestimates the service life. He considered the interaction between many processes, namely CO_2 diffusion, moisture and heat transfer, the mechanism of $CaCO_3$ formation and the availability of $Ca(OH)_2$ in the pore solution due to its transport by water movement. Saetta *et al* **/97/** proposed two dimensional extension of the finite element model to stimulate the diffusion of aggressive substances (CO_2) in concrete.

The rate of carbonation is given by:

$$\delta c/\delta t = v = \alpha_1 \text{ x } f1(h) \text{ x } f_2(g) \text{ x } f_3(c) \text{ x } f_4(T) \qquad (62)$$

α_1 is a non-dimensional parameter.

The rate of reaction depends on the influence of water, carbon dioxide, degree of carbonation c and temperature on the process of calcium carbonate formation.

8.18 O. Burkan Isgor and A. Ghani Razaqpur Model

The following expression was proposed by Papadakis *et al.* **/98/** for the transport of carbon dioxide inside the concrete

$$D_c=1.64\times10^{-6}\,\mu_p(t)^{1.8}(1-h)^{2.2} \qquad (63)$$

where Dc (m^2/s) is the CO_2 diffusion coefficient, h is the relative humidity, expressed as a fraction, at time t and $\mu_p(t)$ is the porosity of the hardened cement paste.

A two-dimensional windows-based finite element program, called CONDUR, was developed to trace the time, moisture and temperature-dependent diffusion of carbon dioxide in concrete. The proposed model involves several field problems such as heat, moisture and CO_2 transport, each of which can be represented by a quasi-harmonic equation of the form

$$\delta/\delta x(k_x\, \delta\Phi/\ \delta x) + \delta/\delta y(k_y\, \delta\Phi/\ \delta y) + Q = \rho c\delta\Phi/\ \delta t \tag{64}$$

In the case of heat transfer, the potential,Φ, represents the temperature, T; and k_x and k_y are the thermal conductivities in x and y directions, respectively. In moisture transfer, the potential,Φ, represents the relative humidity, h; and k_x and k_y are the moisture diffusion coefficients, D_{hx} and D_{hy}, respectively. Similarly, in the case of CO_2 diffusion, the potential represents the concentration of CO_2 and k_x and k_y are the diffusion coefficients in the x and y, respectively. The term Q represents the internal generation or consumption of the species or quantity of interest, ρ and c are pertinent material properties. In the case of heat transfer analysis ρ is the density of the medium and c is its specific heat. The results of the proposed method of analysis agree well with available experimental data from one-dimensional CO_2 diffusion tests. One-dimensional models, which are widely used to investigate CO_2 penetration into concrete, have limited applicability because they are unable to capture the effects of imperfections and variability in concrete properties or local exposure conditions. The finite element method can easily model discrete cracks, while smeared or micro-cracks can be accounted for via the material transport properties. However, further studies are needed to define mass transport properties of cracks.

9.0 SUMMARY

This review of the various aspects of degradation of concrete and corrosion of reinforcement has addressed the following issues:

a) understanding the theory of reinforcement corrosion,
b) elaborating the causative factors responsible for degradation of concrete structures,
c) appreciating the internal (pertaining to the materials) and external (pertaining to the surrounding environment) factors affecting reinforcement corrosion,
d) studying the progresses of corrosion with time and the effects of corrosion on the behavior of the structures and

e) making use of various models and an experimental technique for predicting remaining service life of a corroding RC structure.

10.0 REFERENCES

1. E. Holt, and M. Leivo, Cement and Concrete Composites, 26(5) (2004), 521–530.
2. J. Rottstegge, M. Wilhelm and H.W. Spiess, Cement and Concrete Composites, 28(5) (2006), 417-426.
3. I. Papayianni, G. Tsohos, N. Oikonomou and P. Mavria, Cement and Concrete Composites, 27(2) (2005), 217-222.
4. V. Saraswathy and H.W. Song, Corrosion Reviews, 24(1-2) (2006), 87-122.
5. W. Chalee, M. Teekavanit, K. Kiattikomol, A. Siripanichgorn and C. Jaturapitakkul, Construction and Building Materials, 21(5) (2007), 965-971.
6. Ismail Yurtdas, He Peng, Nicolas Burlion and Frédéric Skoczylas, Cement and Concrete Research, 36(7) (2006), 1286-1293.
7. Hüseyin Yiğiter, Halit Yazıcı and Serdar Aydın, Building and Environment, 42(4) (2007), 1770 –1776.
8. Burak Felekoğlu, Selçuk Türkel and Bülent Baradan, Building and Environment, 42(4) (2007), 1795 –1802.
9. M. Lion, F. Skoczylas, Z. Lafhaj and M. Sersar, Cement and Concrete Research, 35(10) (2005),1937-1942.
10. Lucia Alarcon-Ruiz, Gerard Platret, Etienne Massieu and Alain Ehrlacher, Cement and Concrete Research, 35(3) (2005), 609-613.
11. H. Castro, C. Rodriguez, F.J. Belzunce and A.F. Canteli, Journal of Materials Processing Technology, 143-144 (2003), 134-137.
12. Mamdouh Elbadry and Omer Elzaroug, Composite Structures, 64(1) (2004), 37-45.
13. Abdolkarim Abbasi and Paul J. Hogg, Composites Part B: Engineering, 36(5) (2005), 394-404.
14. A. Abbasi and P.J. Hogg, Composites Part A: Applied Science and Manufacturing, 37(8) (2006), 1142-1150.
15. Anon., ACI Committee 222, "Corrosion of Metals in Concrete". 1996.
16. James M. Gaidis, Cement and Concrete Composites, 26(3) (2004), 181-189.
17. M.F. Montemor, A.M.P. Simoes & M.G.S. Ferreira, Cement and Concrete Composites, 25(4-5) (2003), 491 – 502.

18. M. Ormellese, M. Berra, F. Bolzoni and T. Pastore, Cement and Concrete Research, 36(3) (2006), 536-547.
19. V.N. Shah and C.J. Hookham, Nuclear Engineering and Design, 185(1) (1998), 51 – 81.
20. I.L. Kondratova and T.W. Bremner, Cement and Concrete Research, 34(4) (2004), 603 – 609.
21. Maher A. Bader, Cement and Concrete Composites, 25(4-5) (2003), 539 – 548.
22. Pa Pa Win, Makiko Wantanabe and Atsuhiko Machida, Cement and Concrete Research, 34(7) (2004), 1073 – 1079.
23. Vivian, H.E (1951) Studies in cement aggregate reaction. XVI Aust. J. Appl. Sci. 2, 108 –113.
24. Dent-Glasser, L.S and Kataoka, N, in: Proceedings of The Fiftieth International Conference on Alkali-Aggregate Reaction in Concrete. S 252/23, (1981) 1-7.
25. Concrete Society, Alkali-silica reaction, minimizing the risk of damage to concrete. Guidance notes and model specification clauses. Technical report No. 30, (1987)
26. D.W.S. Ho and R.K. Lewis, Cement and Concrete Research 17 (1987), 489–504.
27. Tahir Gonen and Salih Yazicioglu, Construction and Building Materials 21(5) (2007), 1040-1045.
28. D.R. Moorehead, Cement and Concrete Research, 16(5) (1986), 700–708.
29. Alexander Steffens, Dieter Dinkler and Hermann Ahrens, Cement and Concrete Research, 32(6) (2002), 935-941.
30. L. De Ceukelaire and D. Van Nieuwenburg, Cement and Concrete Research, 23(2) (1993), 442–452.
31. W.P.S. Dias, Cement and Concrete Research 30(8) (2000), 1255–1261.
32. V.G. Papadakis, C.G. Vayenas and M.N. Fardis, ACI Mater. J. 88(1991), 363–373.
33. V.T. Ngala and C.L. Page, Cement and Concrete Research. 27(7) (1997), 995–1007.
34. T. Ishida, M. Soltani and K. Maekawa, Proceedings of the 4th International Conference on Concrete Under Severe Conditions, Seoul, Korea (2004), 205–212.
35. T. Van Gervan, D. Van Baelen, V. Dutree and Vandecasteele, Cement and Concrete Research 34(1) (2004), 149–156.
36. Ha-Won Song, Seung-Jun Kwon, Keun-Joo Byun and Chan-Kyu Park, Cement and Concrete Research, 36(5) (2006), 979-989.

37. Vladimir Zivica, Bull. Mater. Sci., 26(6) (2003), 605-608.
38. J.H. Cahyadi and T. Uomoto, "Influence of environmental relative humidity on carbonation of concretre (mathematical modeling)". In: S. Nagataki et al., Durability of Building Materials and Components 6, E & FN Spon (1993), pp. 1142–1151.
39. J.D. Mozer et al, J. Am. Concr. Inst. (1965), 909–931.
40. ASTM C: 1152- Standard Test Method for Acid-Soluble Chloride in Mortar and Concrete 1990:609–10.
41. C. Arya, N.R. Buenfeld and J.B. Newman, Cement and Concrete Research, 17 (1987), 907–918.
42. B.B. Hope and K.C. Alan Ip, ACI Mater. J. 84 (1987), 306–314.
43. Rasheeduzzafar, ACI Mater. J. 89(6) (1992), 574–586.
44. Rasheeduzzafar, F.H. Dakhil, A.S. Al-Gahtani, S.S. Al-Saadoun and M.A. Bader, ACI Mater. J. 87(2) (1990), 114–122.
45. C. Jaegermann, ACI Mater. J. 87(4) (1990), 333–339.
46. D.W.S. Ho and R.K. Lewis, Cement and Concrete Research 17(1987), 489–504.
47. K. Kobayashi and K. Suttoh, Cement and Concrete Research 21(1991), 273–284.
48. S. Goto and D.M. Roy, Cement and Concrete Research 11(4) (1981), 575 - 579.
49. S.S. Al-Saadoun, Rasheeduzzafar and A.S. Al-Gahtani, The Arab. J. Sci. Eng. 17 (1) (1992), 17–33.
50. Maslehuddin M. "Optimization of Concrete Mix Design for Durability in the Eastern Province of Saudi Arabia", M.Sc. Thesis, Department of Civil Engineering, King Fahd University of Petroleum and Minerals, Dhahran; 1981
51. Arnie Rosenberg, Manufactured Concrete Magazine, 1999, 30 –35.
52. Zoubeir Lafhaj, Marc Goueygou, Assia Djerbi and Mariusz Kaczmarek, Cement and Concrete Research, 36 (4) (2006), 625-633.
53. IS: 3085-1965, "Indian Standard – Method of Test for Permeability of Cement Mortar and Concrete", Bureau of Indian Standards, New Delhi, (1965).
54. J.M. Gaidis, Cement and Concrete Composites, 26 (2004), 181–189.
55. V.S. Ramachandran, Concrete Admixtures Handbook, Noyes Publications, Park Ridge, NJ, USA (1984), 540–545.
56. R.J. Craig and L.E. Wood, Effectiveness of Corrosion Inhibitors and their Influence on the Physical Properties of Portland Cement Mortars, Highway Research Records, 328 (1970), 77.

57. K.W.J. Treadaway and A.D. Russel, In: Highways and Public Works, (36) (1968) 40.
58. A.M. Rosenberg, J.M. Gaidis, T.G. Kossivas and R.W. Previte, in Chloride Corrosion Of Steel In Concrete ASTM STP 629, D.E. Tonini and S.W. Dean Jr., Eds, American Society for Testing of Metals, (1977), 89–99.
59. N.S. Berke, Effects of calcium nitrite and mix design on the corrosion resistance of steel in concrete (Part 2, long-term results). In: Corrosion of Metals in Concrete, NACE, Houston, (1987), 134.
60. N.S. Berke and K.M. Sundberg, In: Proceedings, Paul Krieger, Symposium on Performance of Concrete. ACI SP-122, (1990). 269.
61. V. Saraswathy, Ha–Won Song, Building and Environment, 42(1) (2007), 464-472.
62. Shiyuan Qian and Daniel Cusson, Cement and Concrete Composites, 26(3) (2004), 217-233.
63. W.D. Collins, R.E. Weyers and I.L. Al-Qadi, Corrosion 49(1) (1993), 74.
64. H. Saricimen, M. Mohammad, A. Quddus, M. Shameen & M.S. Barny, Cement and Concrete Composites, 24(1) (2002), 89-100.
65. J.S. MeHattie, I.L. Perez, J.A. Kehr, Cement and Concrete Composites, 18(2) (1996), 93 – 103.
66. K.K. Asthana, L.K. Aggarwal and Rajni Lakhani, Cement and Concrete Research, 29(10) (1999), 1541-1548.
67. IS 13620-1993, Fusion Bonded Epoxy Coated Reinforcing Bars—Specification, 1993.
68. E.G. Sherrwood & K.A. Soudki, Composites Part B Engineering, 31(6-7) (2000), 453-459.
69. G. Batis, N. Kouloumbi, P. Pantazopoulou, Cement and Concrete Composites, 27(2) (2005), 261-267.
70. R. Vedalakshmi, K. Kumar, V. Raju and N.S. Rengaswamy, Cement and Concrete Composites, 22(6) (2000), 417-421.
71. N.S. Rengaswamy, S. Srinivasan and T.M. Balasubramaniyan, Trans SAEST, 23 (2&3) (1988), 162–173.
72. N.S. Rengaswamy, R. Vedalakshmi and K. Balakrishnan, Anticorrosion Meth Mater., 42(3) (1995), 7–10.
73. A. Sanjurjo, Samson Hettiarachchi, K.H. Lau, Philip Cox and Bernard Wood, Surface and Coatings Technology, 54/55 (1992), 224-228.
74. P. Gu, B. Arsenault, J.J. Beaudoin, J.-G. Legoux, B. Harvey and J. Fournier, Cement and Concrete Research, 28(3) (1998), 321-327.

75. S.X. Wang, W. W. Lin, S.A. Ceng and J.Q. Zhang, Cement and Concrete Research, 28(5) (1998), 649-653.
76. R.N. Swamy, S. Koyama, T.Arai and N. Mikami, Durability of Steel Reinforcement in marine environment, SP – 109 "Concrete in Marine Environment" for Concrete Reinforcing Steel Institute (CRSI).
77. D.J. Naus, C.B. Oland, B.R. Ellingwood, C.J. Hookham, H.L. Graves III, Nuclear Engineering and Design, 194 (1999), 73 – 96.
78. Tsuneki I Chikawa and Hitoshi Koizumi, Journal of Nuclear Science and Technology, 39(8) (2002), 880-884.
79. W.E.Norris, D.J.Naus, H.L.Graves III., Nuclear Engineering and Design, 192 (1999), 303 – 329.
80. K. Tuutti, Corrosion of Steel in Concrete, Swedish Cement and Concrete Research Institute, Stochkolm, (1982).
81. P.D. Cady, and R.E. Weyers, Cement, Concrete and Aggregate 5(2) (1983), 81-87.
82. Z.P. Bazant, Journal of the Structural Division, 1979, 1137-1153.
83. S. Morinagn, "Prediction Of Service Lives Of Reinforced Concrete Buildings Based On Rate Of Corrosion Of Reinforcing Steel", Special report of the Institute of Technology, Skimiza Corporation, Japan, (1989).
84. X.M. Wang and H.Y. Zhao, The residual service life prediction of R.C. structures, In: S. Nagataki et al. Durability of Building Materials and Components 6, E & FN Spon (1993), pp. 1107–1114.
85. H.J. Dagher and S. Kulendran, ACI Struct. J., 89(6) (1992), 699–708.
86. Shamsad Ahmad, Cement and Concrete Composites, 25(4-5) (2003), 459-471.
87. Marios Chryssanthopoulos and Garry Sterritt, in Proc of ASRANet International Colloquium - asranet.com (held in Universities of Glasgow & Strathclyde, March 24 – 26 March 2003).
88. O. Klinghoffer, T. Frølund, and E. Poulsen, Rebar Corrosion Rate Measurements For Service Life Estimates, ACI Fall Convention 2000, Toronto, Canada, Committee 365 "Practical Application Of Service Life Models".
89. Koji Takewaka, Toshinobu Yamaguchi and Satoshi Maeda, Journal of Advanced Concrete Technology 1(2) (2003), 139 – 146.
90. Youping Liu, Modeling The Time-to-Cracking of the Cover Concrete in Chloride Contaminated Reinforced Concrete Structures, PhD Thesis, Virginia State University, Blacksburg, Virginia 1996.
91. B. Capra and J.P. Bournazel, Cement and Concrete Research, 28(2) (1998), 251-260.

92. Bruno Capra and Alain Sellier, Mechanics of Materials, 35(8) (2003), 817 – 830.
93. M.C.R. Farage, J.L.D. Alves and E.M.R. Fairbairn, Cement and Concrete Research, 34(3) (2004), 495-505.
94. A. Hillerborg, M. Modeer and P.E. Peterson, Cement and Concrete Research, 6 (6) (1976), 773–782.
95. Z.P. Bazant and B.H. Oh, ACI Mater. Struct., 16(93) (1983), 155–177.
96. Anders Lindvall, 2nd International PhD Symposium in Civil Engineering 1998, Chalmers University of Technology, Sweden.
97. Anna V. Saetta and Renato and V. Vitaliani, Cement and Concrete Research, 34(4) (2004), 571 – 579.
98. O. Burkan Isgor and A. Ghani Razaqpur, Cement and Concrete Composites, 26(1) (2004), 57-73